

Glutathione reductase *gsr-1* is an essential gene required for *Caenorhabditis elegans* early embryonic development

José Antonio Mora-Lorca^{a,b}, Beatriz Sáenz-Narciso^c, Christopher J. Gaffney^d, Francisco José Naranjo-Galindo^{a,1}, José Rafael Pedrajas^e, David Guerrero-Gómez^a, Agnieszka Dobrzynska^f, Peter Askjaer^f, Nathaniel J. Szewczyk^d, Juan Cabello^{c,*}, Antonio Miranda-Vizuete^{a,*,2}

^a Instituto de Biomedicina de Sevilla, Hospital Universitario Virgen del Rocío/CSIC/Universidad de Sevilla, 41013 Sevilla, Spain

^b Departamento de Farmacología, Facultad de Farmacia, Universidad de Sevilla, 41012 Sevilla, Spain

^c Center for Biomedical Research of La Rioja (CIBIR), 26006 Logroño, Spain

^d MRC/ARUK Centre for Musculoskeletal Ageing Research, University of Nottingham and Medical School Royal Derby Hospital, DE22 3DT Derby, United Kingdom

^e Grupo de Bioquímica y Señalización Celular, Departamento de Biología Experimental, Universidad de Jaén, 23071 Jaén, Spain

^f Andalusian Center for Developmental Biology (CABD), CSIC/JA/Universidad Pablo de Olavide, 41013 Seville, Spain

ARTICLE INFO

Article history:

Received 28 March 2016

Accepted 18 April 2016

Available online 24 April 2016

Keywords:

Caenorhabditis elegans

Embryonic development

Glutathione reductase

Mitochondria

Redox

ABSTRACT

Glutathione is the most abundant thiol in the vast majority of organisms and is maintained in its reduced form by the flavoenzyme glutathione reductase. In this work, we describe the genetic and functional analysis of the *Caenorhabditis elegans gsr-1* gene that encodes the only glutathione reductase protein in this model organism. By using green fluorescent protein reporters we demonstrate that *gsr-1* produces two GSR-1 isoforms, one located in the cytoplasm and one in the mitochondria. *gsr-1* loss of function mutants display a fully penetrant embryonic lethal phenotype characterized by a progressive and robust cell division delay accompanied by an aberrant distribution of interphasic chromatin in the periphery of the cell nucleus. Maternally expressed GSR-1 is sufficient to support embryonic development but these animals are short-lived, sensitized to chemical stress, have increased mitochondrial fragmentation and lower mitochondrial DNA content. Furthermore, the embryonic lethality of *gsr-1* worms is prevented by restoring GSR-1 activity in the cytoplasm but not in mitochondria. Given the fact that the thioredoxin redox systems are dispensable in *C. elegans*, our data support a prominent role of the glutathione reductase/glutathione pathway in maintaining redox homeostasis in the nematode.

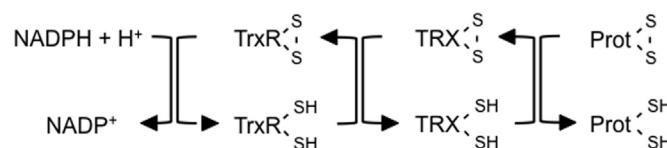
© 2016 Elsevier Inc. All rights reserved.

1. Introduction

Maintenance of thiol redox homeostasis is crucial for survival and the thioredoxin and glutaredoxin systems are the two main pathways that control the redox status in virtually all organisms [1]. The thioredoxin system is composed of thioredoxin reductase (TrxR) and thioredoxins (Trx) while the glutaredoxin system comprises glutathione reductase (GR), glutathione (GSH) and glutaredoxins (Grx), where thioredoxins and glutaredoxins operate as terminal oxidoreductases using the reducing power of

NADPH [2]. These two systems are mechanistically and structurally very similar, regulating the formation of disulfides within and between proteins, with the main difference being the use of the tripeptide glutathione (L-γ-glutamyl-L-cysteinyl-glycine) as electron donor for glutaredoxins in the glutaredoxin system. In addition, the glutaredoxin system also catalyzes the formation of disulfides between proteins and GSH, namely glutathionylation, which has been shown to be an important post-translational modification, modulating the activity of many proteins [3].

Thioredoxin system



* Corresponding authors.

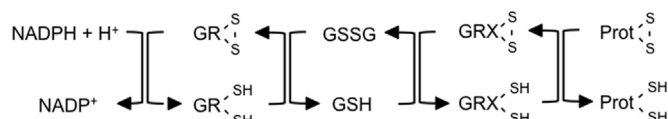
E-mail addresses: juan.cabello@riojasalud.es (J. Cabello),

amiranda-ibis@us.es (A. Miranda-Vizuete).

¹ Present address: Functional Genomics and Proteomics, Department of Biology, KU Leuven, 3000 Leuven, Belgium.

² Equal senior author contribution.

Glutaredoxin system



GSH is found in cyanobacteria, proteobacteria and some gram-positive bacteria as well as most eukaryotes [4]. Inactivating mutations in the gene encoding γ -glutamylcysteine synthetase, the enzyme that catalyzes the first step in GSH synthesis, are lethal in all organisms studied from yeast to mammals, including plants [5–9] highlighting the physiological relevance of GSH in these organisms. Moreover, mutations in the gene encoding glutathione synthetase, that catalyzes the second, final step of GSH synthesis, are also lethal in *Arabidopsis thaliana* [10] and *Mus musculus* [11] while they are viable in *Saccharomyces cerevisiae* [12] and *Drosophila melanogaster* [13]. In these latter organisms, it has been proposed that the intermediate γ -glutamyl-cysteine, which accumulates in glutathione synthetase mutants, substitutes for GSH to allow growth. Of note, although the *C. elegans* glutathione synthetase ortholog, *gss-1*, has not been yet characterized, a *gss-1* (*tm672*) deletion mutant has been reported as lethal/sterile by the NBRP *C. elegans* Gene Knockout Consortium (<http://www.shigen.nig.ac.jp/c.elegans/>).

The lethal phenotype of GSH synthesis mutants contrasts with the dispensability, in the vast majority of eukaryotes, of the glutathione reductase gene that encodes the enzyme that recycles reduced GSH from its oxidized form GSSG. This inessentiality of glutathione reductase for normal growth and development is explained by the thioredoxin system being able to reduce GSSG, a trait that is conserved from bacteria to mammals [14] and also by either accumulating GSSG in yeast vacuole [15] or by excreting GSSG in mammalian cells [16]. Exceptions to glutathione reductase dispensability are the fission yeast *Schizosaccharomyces pombe* [17], the *Plasmodium berghei* parasite in its mosquito oocyst stage but not in the blood stage [18] and the *A. thaliana* GR2 gene, encoding a chloroplastic/mitochondrial glutathione reductase whose inactivation causes early embryonic lethality [19]. The lethality of *A. thaliana* GR2 mutants is most likely due to a deficiency in chloroplasts function, as in this organism mitochondrial thioredoxin reductase TRXR2 is able to reduce GSSG in mitochondria (Meyer AJ, personal communication). In addition, *D. melanogaster* (and probably other insects) lacks a *bona fide* glutathione reductase gene and the reduction of GSSG is performed by the thioredoxin system, which is essential in this organism [20].

All eukaryotic organisms relying on glutathione metabolism have two distinct pools of glutathione reductase activity located in cytoplasm and mitochondria, respectively (with the exception of photosynthetic organisms that also have glutathione reductase activity in chloroplasts and peroxisomes [21]). In most cases, one single gene encodes both cytoplasmic and mitochondrial glutathione reductase isoforms by the use of alternative translation initiation sites [22–25]. Whereas in *Escherichia coli* the thioredoxin and glutathione systems are functionally redundant in maintaining redox homeostasis [26], important differences on their respective contribution to the redox status of the different

subcellular compartments have been identified in eukaryotic organisms, mainly through work in yeast and mammals. Hence, the yeast thioredoxin system controls the thiol redox status in the cytoplasm where the glutathione system acts merely as a backup. In contrast, the glutathione system is the dominant system to maintain thiol redox control in yeast mitochondria [27–29]. In mammals, knock-out mice lacking glutathione reductase are viable [30] while inactivation of the components of the cytoplasmic and mitochondrial thioredoxin systems causes embryonic lethality in mice [31–34], initially suggesting that the mammalian thioredoxin system may have a predominant role in maintaining redox homeostasis. However, studies on mice harboring conditional alleles of cytosolic thioredoxin reductase TrxR1 to bypass embryonic lethality demonstrate that TrxR1-null mice and cells are robustly viable, relying on the glutathione pathway for survival [35,36]. Indeed, mice lacking both TrxR1 and glutathione reductase in all hepatocytes sustain hepatic redox homeostasis and organismal survival, through *de novo* GSH synthesis via the transsulfuration pathway using dietary methionine as cysteine precursor [16]. Together, these data in mammals uphold a more prominent role of the glutathione pathway on maintaining redox homeostasis while the thioredoxin system appears to play key functions during embryonic development.

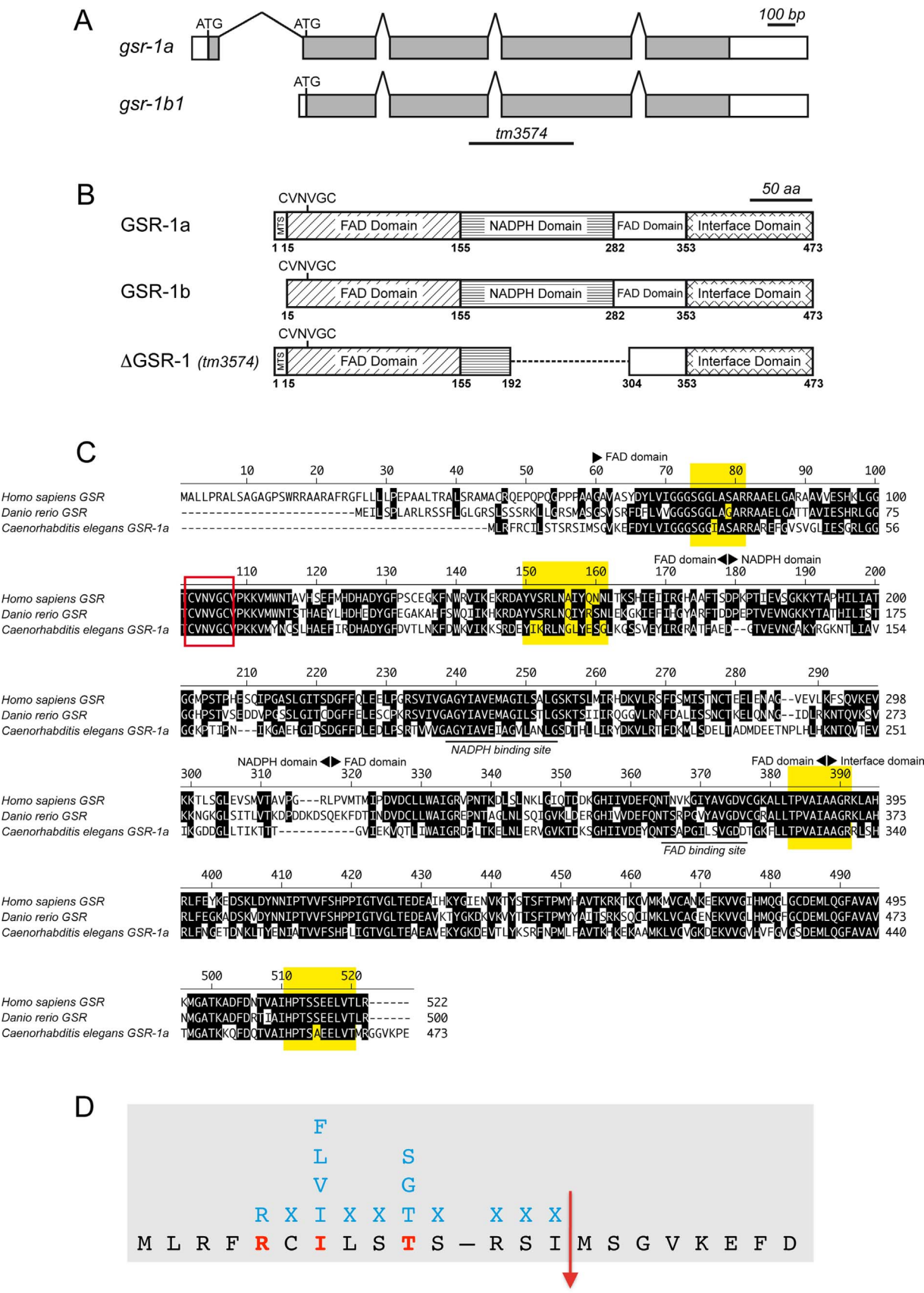
In contrast to mammals, the *C. elegans* thioredoxin system is dispensable for embryonic and postembryonic development, as mutants lacking both cytoplasmic and mitochondrial thioredoxin reductases, *trx-1* and *trx-2*, are viable and reach adulthood indistinguishably from wild type controls [37,38], supporting the idea that the glutathione system is also responsible for maintenance of redox homeostasis in worms. Lüersen et al. have shown that the *C. elegans* *gsr-1* gene encodes a functional glutathione reductase protein [39], which is required for survival to paraquat and juglone treatments. In this work, we demonstrate that the *C. elegans* *gsr-1* gene encodes both cytoplasmic and mitochondrial glutathione reductase isoforms and that is required for embryonic development. This lethal phenotype of *gsr-1* mutants arises from a specific requirement of the enzyme in the cytoplasm, the subcellular compartment where GSH is synthesized. In contrast, *gsr-1* mutants maternally expressing GSR-1 are able to develop normally but are sensitized to stress, are short-lived and have compromised mitochondria.

2. Results

2.1. *C. elegans* GSR-1 is widely expressed and is targeted to both cytoplasm and mitochondria

The *gsr-1* locus is organized into 5 exons and 4 introns and expresses two main mRNA variants, *gsr-1a* and *gsr-1b1* (Fig. 1A), whose conceptual translation results into two different isoforms, GSR-1a and GSR-1b, with the former having an additional 14 amino acid N-terminal extension (Fig. 1B). Two other minor mRNA variants have been reported, *gsr-1b2* and *gsr-1b3*, which differ only in the sequence of their respective 5'-UTRs but also generate the GSR-1b isoform (<http://www.wormbase.org/>). *C. elegans* GSR-1 is

Fig. 1. *gsr-1* mRNA and protein analysis. (A) Schematic representation of the two main *gsr-1* mRNA variants. Boxes represent exons and lines show spliced introns. White boxes indicate 5'-UTR and 3'-UTR, respectively, and grey boxes indicate the ORF. The region of the *gsr-1* mRNA missing in the *gsr-1(tm3574)* deletion allele is underlined. (B) Protein domain organization of GSR-1a and GSR-1b isoforms as well as that of the truncated Δ GSR-1 protein resulting from translation of the *gsr-1(tm3574)* allele. Numbers indicate the amino acid residues flanking the different protein domains, based on the domain organization reported for the human GSR orthologue [80]. (C) Sequence alignment of *C. elegans* GSR-1 with the corresponding human and zebrafish GSR orthologues. The red rectangle indicates the conserved redox active site CVNVC. The yellow boxes highlight the residues involved in GSSG binding [81]. The NADPH and FAD binding sites are underlined. Identical residues are shown in black. The numbers on the left indicate the respective amino acid residue. The different domains boundaries are indicated above the sequences and are inferred from comparison with those reported for human GSR protein [80]. (D) Sequence of the GSR-1a mitochondrial targeting sequence (MTS). Amino acid residues matching the two matrix protease model (in blue. X, any amino acid residue) [41] are highlighted in red. The MTS cleavage site is indicated by the upside-down arrow. The residues encoded by *gsr-1* first and second exons are separated by an hyphen. (For interpretation of the references to color in this figure legend, the reader is referred to the web version of this article.)



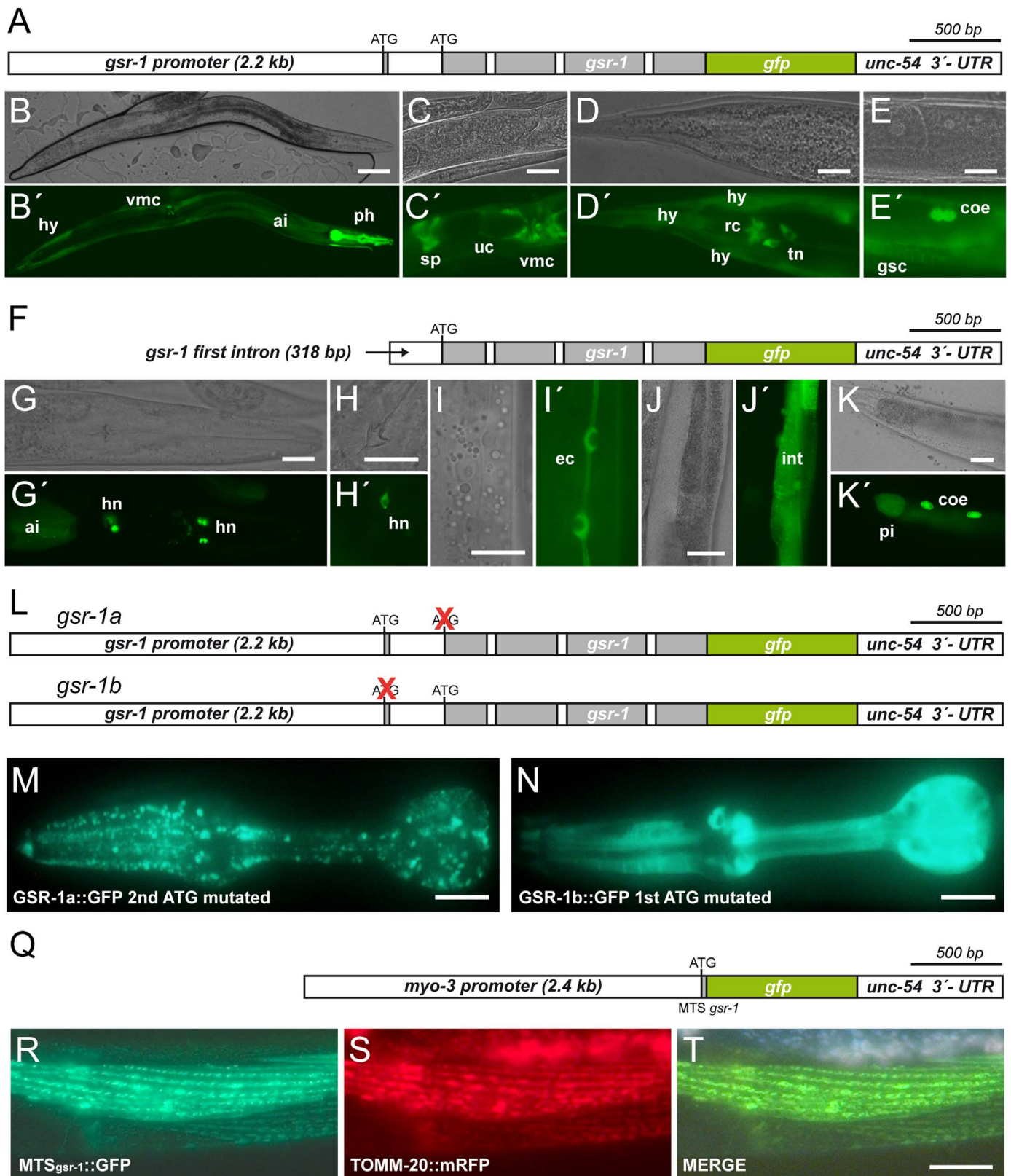


Fig. 2. GSR-1 tissue, cellular and subcellular expression analysis. (A) Scheme of the GSR-1 translational GFP fusion construct used to determine expression from *gsr-1* upstream promoter. Exons are in grey boxes and introns in white boxes. (B–E) Differential interference contrast and (B'–E') fluorescence images of transgenic worms expressing the *Pgsr-1::gsr-1::gfp* construct; ai, anterior intestine; coe, coelomocytes; gsc, gonad sheet cell; hy, hypodermis; ph, pharynx; rc, rectal cells; sp, spermatheca; tn, tail neurons; uc, uterine cells; vmc, vulva muscle cells. (F) Scheme of the GSR-1 translational GFP fusion construct used to determine expression from *gsr-1* first intron. Exons are in grey boxes and introns in white boxes. (G–K) Differential interference contrast and (G'–K') fluorescence images of transgenic worms expressing the *Pgsr-1::gsr-1::gfp* construct; ai, anterior intestine; coe, coelomocytes; ec, excretory cell; hn, head neurons; int, intestine; pi, posterior intestine. (L) Schemes of the GSR-1 translational GFP fusion constructs used to determine subcellular localization of GSR-1a and GSR-1b isoforms. Red X indicates the mutated ATG codon. Exons are in grey boxes and introns in white boxes. (M) Dotted fluorescence labeling in pharynx of transgenic worms expressing the *Pgsr-1::gsr-1::gfp* construct with the second ATG codon mutated. (N) Diffuse cytoplasmic fluorescence labeling in pharynx of transgenic worms expressing the *Pgsr-1::gsr-1::gfp* construct with the first ATG codon mutated. (Q) Scheme of the construct used to determine GSR-1a MTS functionality when fused to GFP under the control of the *myo-3* muscle promoter. GSR-1a MTS is shown in a grey box. Fluorescence images of muscle cells of transgenic worms expressing (R) the *Pmyo-3::MTS_gsr-1::gfp* construct, (S) the *Pmyo-3::tomm-20::mrfp* construct and (T) merged picture showing colocalization in muscle tubular mitochondria. Scale bar 20 μ m in all images except 100 μ m in B. Note Images B–K and M–T were taken with different microscopes and settings (see Section 4.2).

highly homologous through all protein domains to vertebrate glutathione reductases, including the conserved redox active site CVNVGC (Fig. 1B–C). The GSR-1a N-terminal extension, mostly encoded by the first *gsr-1* exon, displays characteristics of a mitochondrial targeting sequence (MTS) [40], cleavable by the two matrix protease model (Fig. 1D) [41]. This predicts that GSR-1a is located in the mitochondrial matrix while GSR-1b, lacking this putative MTS and initiated from a downstream in-frame ATG codon located at the beginning of the second exon (Fig. 1A), is a cytoplasmic protein.

To demonstrate this dual subcellular localization *in vivo* as well as to describe the tissue and cellular expression pattern of both GSR-1 isoforms in detail, we first generated transgenic worms expressing a translational GFP fusion spanning a 2.2 kb fragment of the *gsr-1* promoter plus the complete *gsr-1* genomic ORF (Fig. 2A). These transgenic animals showed strong fluorescence in pharynx while weaker labeling was found in hypodermis, intestine, vulva muscle cells, spermatheca, uterine cells, coelomocytes, gonad sheath cells, rectal cells and a couple of unidentified neurons (probably PVPL/R) in the tail (Fig. 2B–E). Long first introns have been shown to be important for gene regulation by binding a set of transcription factors different to those binding the upstream promoter [42]. As *gsr-1* exons 1 and 2 are separated by a 318 bp intron, considerably larger than the rest of *gsr-1* introns (Fig. 1A), we set to investigate whether the *gsr-1* first intron also has promoter activity. Interestingly, transgenic worms expressing a translational GFP fusion spanning the *gsr-1* ORF from the first intron (Fig. 2F) show labeling in some neurons in the head, excretory channel, intestine and coelomocytes (Fig. 2G–K). This result suggests that the *gsr-1* first intron possess intrinsic promoter activity, independent from that of the *gsr-1* upstream promoter.

To prove that *C. elegans gsr-1* gene encodes both mitochondrial and cytoplasmic isoforms *in vivo*, we generated transgenic worms expressing the full *gsr-1* translational GFP fusion in which either ATG codon is mutated (Fig. 2L). Thus, inactivation of the second ATG codon forces translation from the first ATG codon resulting in a dotted GFP pattern, consistent with mitochondrial localization (best seen in the pharynx) [43] (Fig. 2M). In turn, when forcing expression from the first ATG codon by inactivation of the second ATG codon, a diffuse GFP labeling indicating a cytoplasmic localization was obtained (Fig. 2N). Similar diffuse fluorescence labeling was found when removing *gsr-1* first exon, which encodes most of GSR-1a MTS (*data not shown*). We further demonstrate that the additional 14 amino acids of GSR-1a constitute a functional MTS on its own as, when expressed in worm muscle cells, the fusion protein MTS*gsr-1*::GFP is found in the typical tubular distribution along the cell longitudinal axis, colocalizing with the TOMM-20::mRFP mitochondrial marker [38] (Fig. 2Q–T). Together, we conclude that the *C. elegans gsr-1* gene encodes both mitochondrial (GSR-1a) and cytoplasmic (GSR-1b) isoforms. In addition, we further refine and expand the *gsr-1* tissue and cellular expression pattern previously reported [37,39].

2.2. *gsr-1* is essential for *C. elegans* embryonic development and *gsr-1(m+,z-)* mutants are sensitized to chemical and developmental stresses and have compromised mitochondria

To investigate GSR-1 function, we used a worm strain carrying the *gsr-1(tm3574)* deletion allele, which spans 383 bp and removes part of *gsr-1* third exon, the third intron and part of the fourth exon (Fig. 1A). Sequencing of *gsr-1(tm3574)* cDNA demonstrates that it encodes an in frame truncated protein (GSR-1Δ193–302, abbreviated as ΔGSR-1) lacking most of the NADPH domain plus a minor fraction of the second FAD domain (Fig. 1B). Using purified recombinant protein expressed in bacteria, we show that wild type GSR-1b is able to reduce GSSG in a dose-dependent

manner while ΔGSR-1b was devoid of enzymatic activity (Fig. 3A), thus confirming *gsr-1(tm3574)* as a loss of function allele most likely by failure to bind NADPH required for redox cycling. GSR-1b did not function as thioredoxin reductase when using either yeast TRX3 or worm TRX-2 as substrates (*data not shown*).

The *gsr-1(tm3574)* allele is reported as lethal/sterile by the NBRP *C. elegans* Gene Knockout Consortium (<http://www.shigen.nig.ac.jp/c.elegans/>). Six times backcrossed *gsr-1(tm3574)* animals retained the lethal phenotype, so the *tm3574* allele was maintained in heterozygosity using GFP or RFP derivatives of the *qC1* balancer [44]. Homozygous *gsr-1* animals segregating from balanced parents (hereafter referred as *gsr-1(m+,z-)*; *m*, maternal and *z*, zygotic), have a normal embryonic and postembryonic development, reaching reproductive stage indistinguishably of wild type controls. Thus, maternally contributed *gsr-1* mRNA and/or GSR-1 protein is enough to allow *gsr-1* mutants to accomplish a normal life cycle. In turn, the *gsr-1(m-,z-)* embryos generated by these animals invariably arrest during embryogenesis.

RNAi downregulation of *gsr-1* expression has been shown to decrease *C. elegans* lifespan, to sensitize worms to the prooxidant juglone and the superoxide anion generator paraquat [39], to impair worm molting in the absence of cytoplasmic thioredoxin reductase *trx-1* gene [37] and to induce *skn-1* target genes such as *gst-4* or *gcs-1* without an obvious nuclear translocation of a *skn-1* GFP reporter [45]. To determine whether the maternal contribution of *gsr-1(m+,z-)* worms is functionally equivalent to the decreased *gsr-1* mRNA levels caused by RNAi, we tested *gsr-1(m+,z-)* individuals in all the above mentioned scenarios. Our data indicate that, indeed, this is the case as *gsr-1(m+,z-)* animals are short-lived (Fig. 3B), are highly sensitive to juglone and paraquat (Fig. 3C), have a fully penetrant larval arrest phenotype in a *trx-1(sv47)* mutant background (Fig. 3D) and induce GST-4 and GCS-1 reporters without significant SKN-1B/C::GFP nuclear translocation (Fig. 3E). Therefore, maternally provided *gsr-1* mRNA and/or GSR-1 protein is enough to allow *gsr-1(m+,z-)* mutants to reach reproductive stage under non-stressed growth conditions but it is insufficient to afford effective protection against stress or developmental constraints.

The extreme sensitivity of *gsr-1(m+,z-)* worms to chemicals that impair mitochondrial function prompted us to assess mitochondrial status in these animals. We found that *gsr-1(m+,z-)* worms have a clear mitochondrial fragmentation phenotype in muscle cells (Fig. 4A) while muscle sarcomere structure is preserved (Fig. 4B). In addition, the mitochondrial membrane potential and total mitochondria content measured by incorporation of the fluorescent dye JC-10 was significantly decreased (Fig. 4C). Moreover, *gsr-1(m+,z-)* worms display a strong induction of the mitochondrial UPR reporter HSP-6::GFP [46] (Fig. 4D), overall indicating that decreased *gsr-1* levels cause mitochondrial stress and dysfunction. As a whole, these results validate the use of *gsr-1(m+,z-)* worms as a tool to investigate the role of GSR-1 in postembryonic development.

2.3. *gsr-1(m-,z-)* embryos arrest at the pregastrula/gastrula stage displaying progressive cell division delay and aberrant interphasic chromatin distribution

Next, we moved to study in detail the *gsr-1(m-,z-)* embryonic arrest phenotype. For this purpose, we video-recorded several *gsr-1(m-,z-)* embryos (*n*=26) and found that they all arrest at the pregastrula/gastrula stage ranging from 17 to 103 cells (Fig. 5A–C and Movies 1–3). This arrest interval is roughly coincidental with the time at which *C. elegans* embryos start expressing a *Pgsr-1::gfp* transcriptional construct (Fig. 5D). Arrested *gsr-1(m-,z-)* embryonic cells are superficially normal for at least the length of normal embryogenesis with no signs of necrosis or apoptosis, as it has

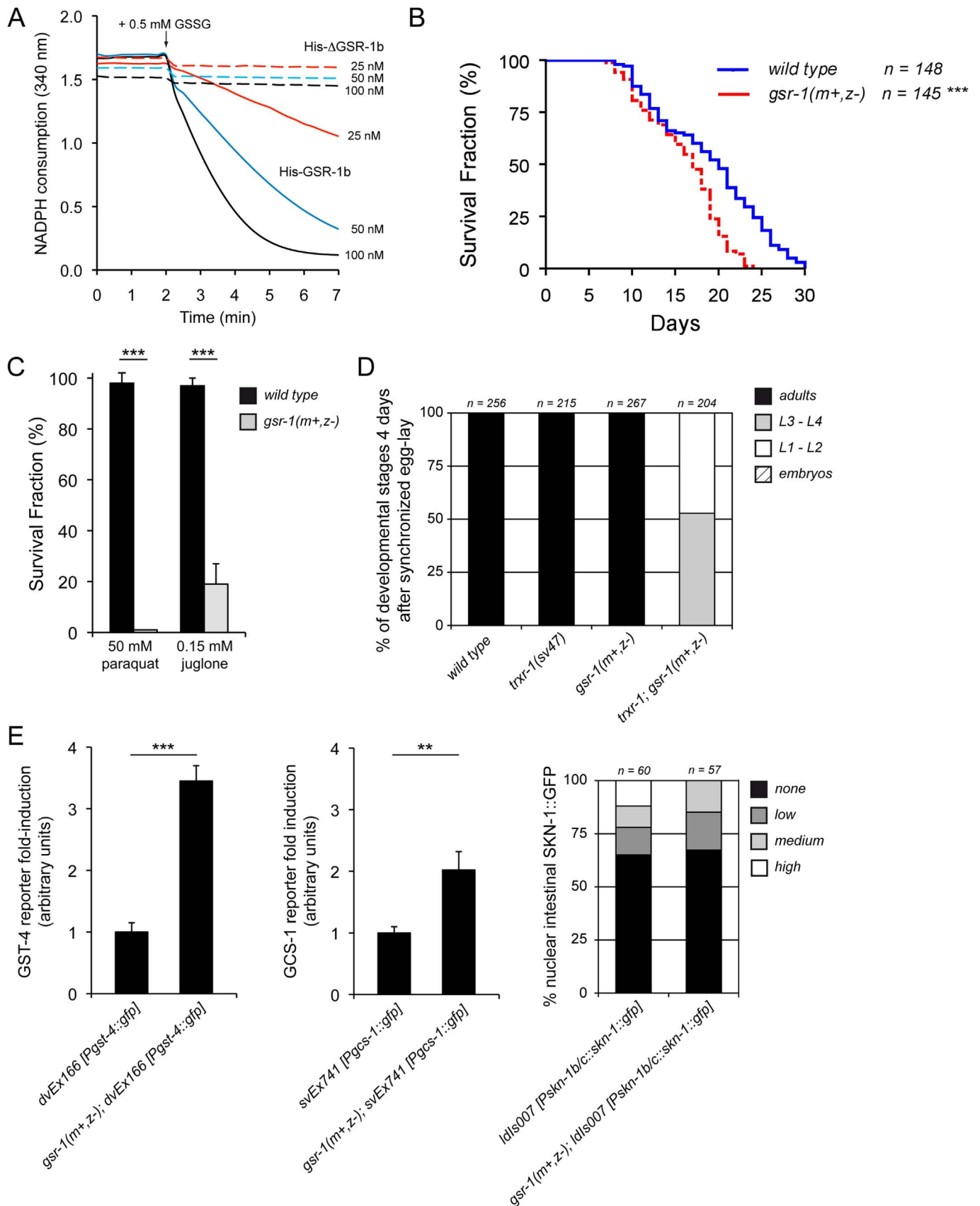


Fig. 3. Glutathione reductase enzymatic activity and phenotypes of $gsr-1(m+,z-)$ mutants. (A) GSSG reductase enzymatic activity of different concentrations of recombinant His-GSR-1b (straight lines) and His-ΔGSR-1b (dashed lines) in the presence of 0.5 mM GSSG and 0.25 mM NADPH. (B) The longevity was assayed at 20 °C in *E. coli* OP50. Kaplan-Meier plot was used to show the fraction of animals that survive over time. Longevity was performed twice, obtaining similar results, and the composite data is shown. The survival rate of $gsr-1(m+,z-)$ animals was compared to that of wild type using the log-rank (Mantel-Cox) test and the differences were found significant (*** $p < 0.001$). (C) Sensitivity of $gsr-1(m+,z-)$ animals to acute paraquat and juglone exposure. Data are the mean \pm SD of four independent experiments with three biological replicates each ($n \geq 200$; *** $p < 0.001$, by unpaired, two-tail Student *t*-test). (D) Percentage of developmental stages of single and double mutants combining the $trx-1(sv47)$ and the $gsr-1(m+,z-)$ mutations. Data are the mean of three independent experiments (n =total number of individuals scored). (E) Induction of GST-4 and GCS-1 transcriptional GFP reporters and percentage of nuclear localization of a SKN-1B/C translational GFP reporter in a $gsr-1(m+,z-)$ background. For GST-4 and GCS-1 reporters, the data are the mean \pm SD of 25 individuals for each genotype (*** $p < 0.001$, ** $p < 0.01$ by unpaired, two-tail Student *t*-test). For SKN-1 reporter the data are from two independent experiments (n =total number of individuals scored).

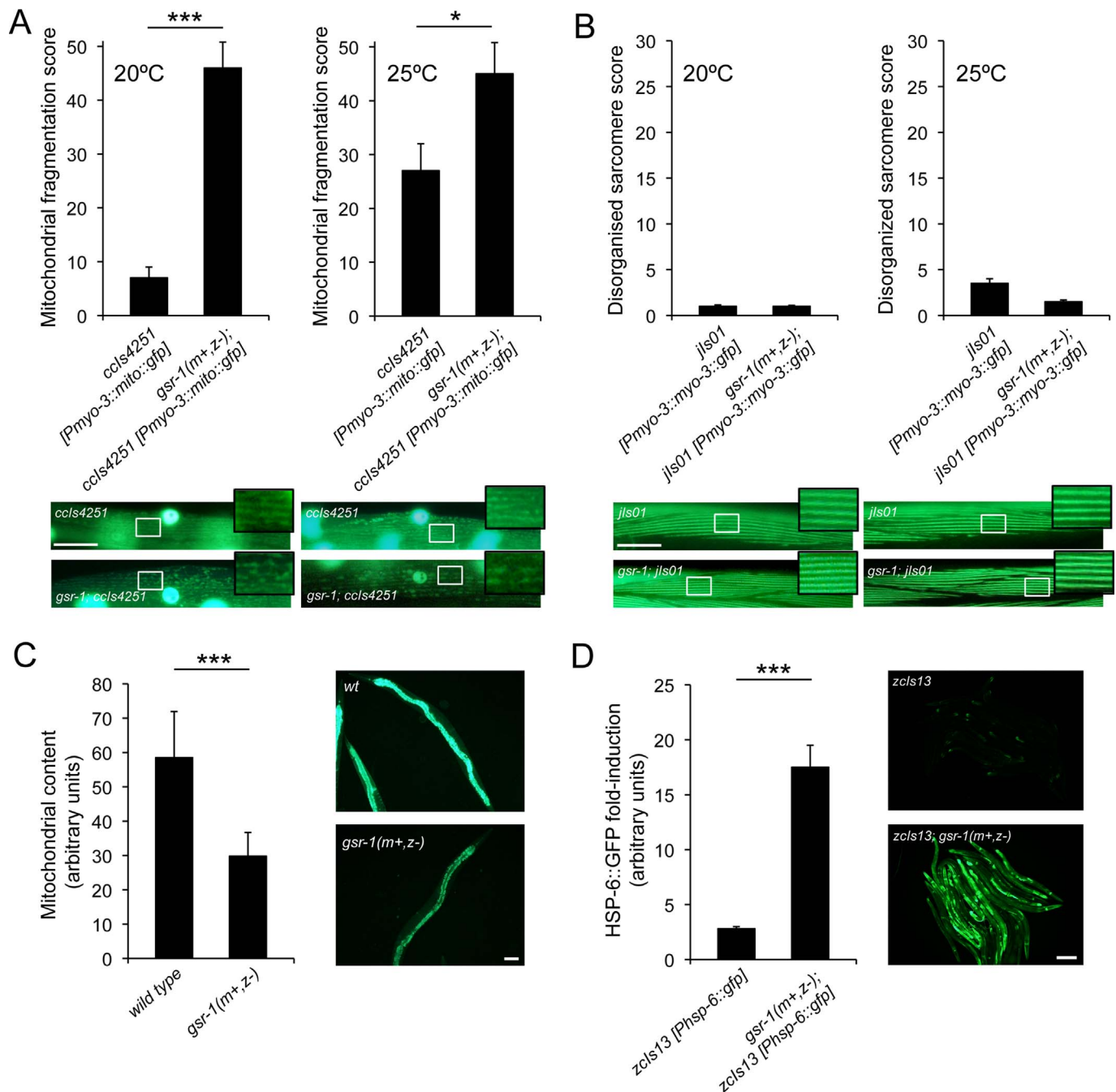


Fig. 4. *gsr-1(m+,z-)* mutants display mitochondrial phenotypes. (A) Increased mitochondrial fragmentation is observed in *gsr-1(m+,z-)* animals expressing the mitochondrial reporter *ccls4251* [Pmyo-3::mito::gfp] in muscle cells. Data are the total \pm SEM of three independent experiments with 20 animals per experiment at 20 °C and 25 °C ($n=60$ total at each temperature) (* $p < 0.05$, *** $p < 0.001$, by a Mann Whitney test). Representative images of each genotype are shown. Scale bar 20 μ m. (B) Muscle cell integrity is not affected in *gsr-1(m+,z-)* worms as demonstrated by the maintenance of sarcomere myotubular structure visualized using the *jls01* [Pmyo-3::myo-3::gfp] reporter. Data are the total \pm SEM of one experiment with 20 animals ($p > 0.05$ by a Mann Whitney test). Representative images of each genotype are shown. Scale bar 20 μ m. (C) Quantification of the total mitochondrial content measured by JC-10 dye incorporation. Data are the average \pm SD of 20 individuals per genotype (*** $p < 0.001$ by a Mann Whitney test). Representative images of each genotype are shown. Scale bar 100 μ m. (D) Mitochondrial UPR is induced in *gsr-1(m+,z-)* worms expressing the reporter *zcls13* [Phsp-6::gfp]. Data are the mean \pm SD of 40 individuals per genotype (*** $p < 0.001$, by unpaired two-tail Student *t*-test). Representative images of each genotype are shown. Scale bar 200 μ m.

been reported for most embryonic lethal mutants [47] (Fig. 5A-C and Movies 1–3). However, cell lineage analysis of *gsr-1(m-,z-)* embryos identifies a dramatic delay of cell divisions timing, already detectable at the first embryonic divisions that is progressively enhanced until complete arrest occurs (Fig. 6A and Supplemental Fig. 1A-C).

We next explored the possible causes of the progressive delay of cell division timing of *gsr-1(m-,z-)* embryos. Among other traits,

mutations in genes impairing mitochondrial function or genes encoding chromatin regulators have been shown to retard cell divisions in *C. elegans* embryos [48,49]. Therefore, we set to investigate whether *gsr-1* mutants impact these two pathways given that mitochondria-associated phenotypes are found in *gsr-1(m+,z-)* animals and because histone 3 glutathionylation destabilizes nucleosome structure and GSH depletion decreases DNA synthesis rate [50].

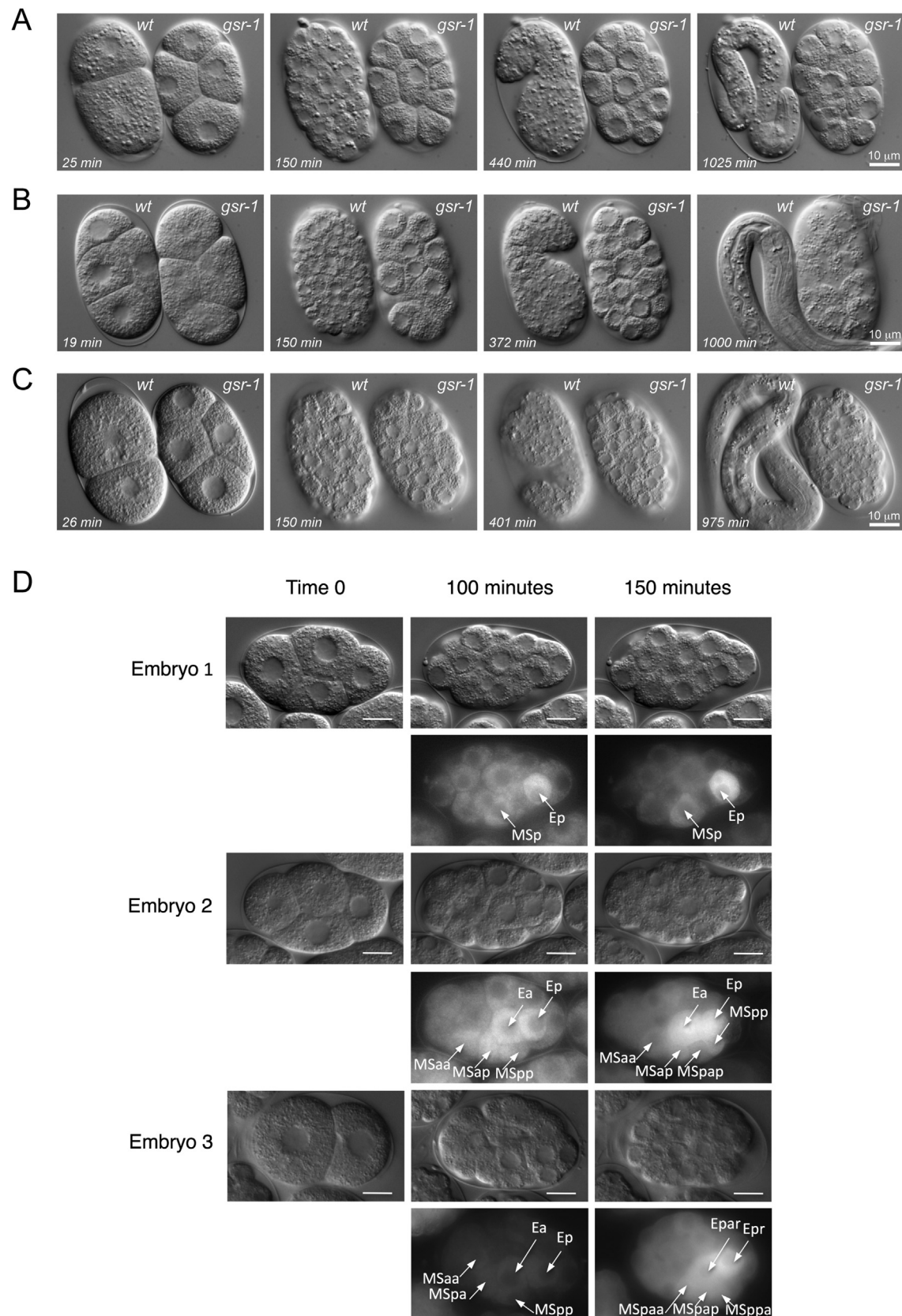


Fig. 5. Identification of the cell-stage time of arrest of *gsr-1(m-z-)* embryos and determination of GSR-1 expression initiation. (A–C) Differential interference contrast still images of developing wild type and *gsr-1(m-z-)* embryos analyzed by 4D-microscopy. Three representative independent experiments are provided, illustrating the cases at which *gsr-1(m-z-)* embryos arrest at the earliest, the latest and an intermediate cell-stage. (A) Arrest at 17 cell-stage; (B) arrest at 33 cell-stage; (C) arrest at 103 cell-stage. *gsr-1* in the images refers to *gsr-1(m-z-)* embryos. (D) Fluorescence and differential interference contrast still images of developing embryos from transgenic animals expressing the transcriptional construct *Pgsl-1::gfp*. Three independent embryos are shown. *gsr-1* expression begins approximately at 100 min since embryos start developing. In these initial stages, *gsr-1* stronger expression is found in E blastomere descendants (intestine precursors) and MS blastomeres descendants (neurons and mesodermic tissues precursors). Scale bar 10 μ m. All analyses were performed at 25 °C.

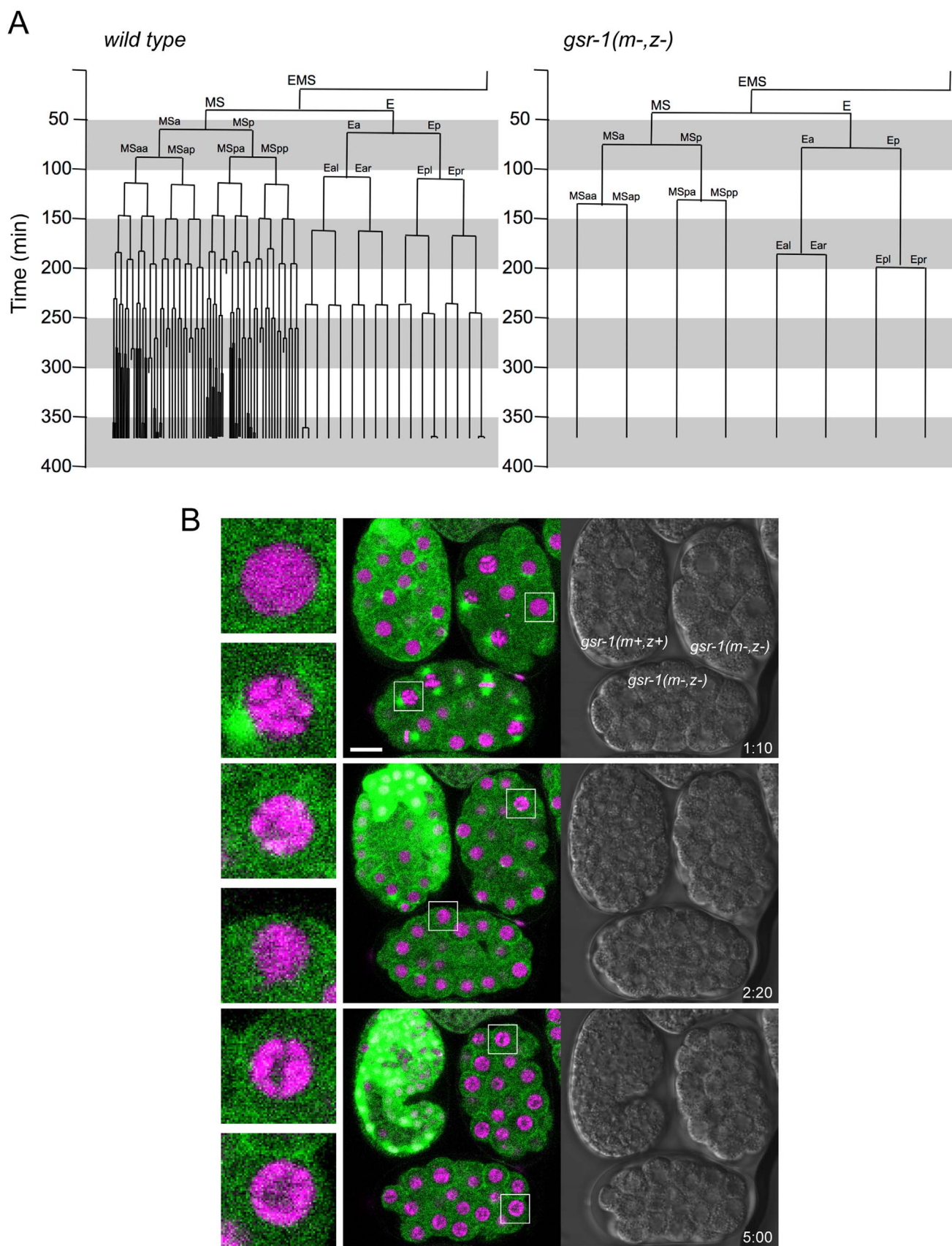


Fig. 6. Cell division delay and progressive perinuclear localization of interphasic chromatin in *gsr-1(m-,z-)* embryos. (A) Cell lineage timing analysis of the EMS blastomere descendants of the *gsr-1(m-,z-)* embryo depicted in Fig. 5B compared to that of wild type embryos. For complete cell lineage analysis, see Supplemental Fig. 1B. (B) *gsr-1(m+,z+)* and *gsr-1(m-,z-)* embryos expressing mCherry::HIS-58 (magenta) and GFP::TBB-2 were observed by live confocal microscopy. Time is indicated in hours: minutes from beginning of recording (see Movie 5). At 2:20 and more evidently at 5:00 chromosomes are condensed at the nuclear periphery of *gsr-1(m-,z-)* embryos. Scale bar 10 μ m.

To evaluate the integrity of the mitochondrial network in *gsr-1(m-,z-)* embryos, we attempted labeling these organelles with rhodamine 6G followed by *in vivo* image analysis [51]. Despite rhodamine 6G efficiently stained embryo mitochondria, no major differences in the dynamics of the mitochondrial network were observed between young wild type and *gsr-1(m-,z-)* embryos (Movie 4). Reduced cell size of older embryos precluded analysis of differentiated embryonic cells. Regarding the other possible cause of cell division delay, we examined chromatin dynamics in *gsr-1(m-,z-)* embryos by time-lapse confocal microscopy. During early development, interphasic chromatin occupied the entire nuclear volume whereas mitotic chromosomes condensed in the

nuclear interior (Fig. 6B and Movie 5; 1:10). However, concomitantly with cessation of cell divisions in *gsr-1(m-,z-)* embryos, a progressive aberrant distribution of chromatin at the nuclear periphery was observed (Fig. 6B and Movie 5; 2:20–5:00). Collectively, these results suggest that *gsr-1* deficiency impacts nuclear chromatin dynamics pointing to a nuclear dysfunction as a possible cause of *gsr-1(m-,z-)* embryonic arrest.

2.4. Cytoplasmic, but not mitochondrial, GSR-1 expression restores viability of *gsr-1(m-,z-)* embryos

The fully penetrant embryonic arrest phenotype of *gsr-1(m-,z-)* embryos is rescued by transgenes expressing wild type GSR-1

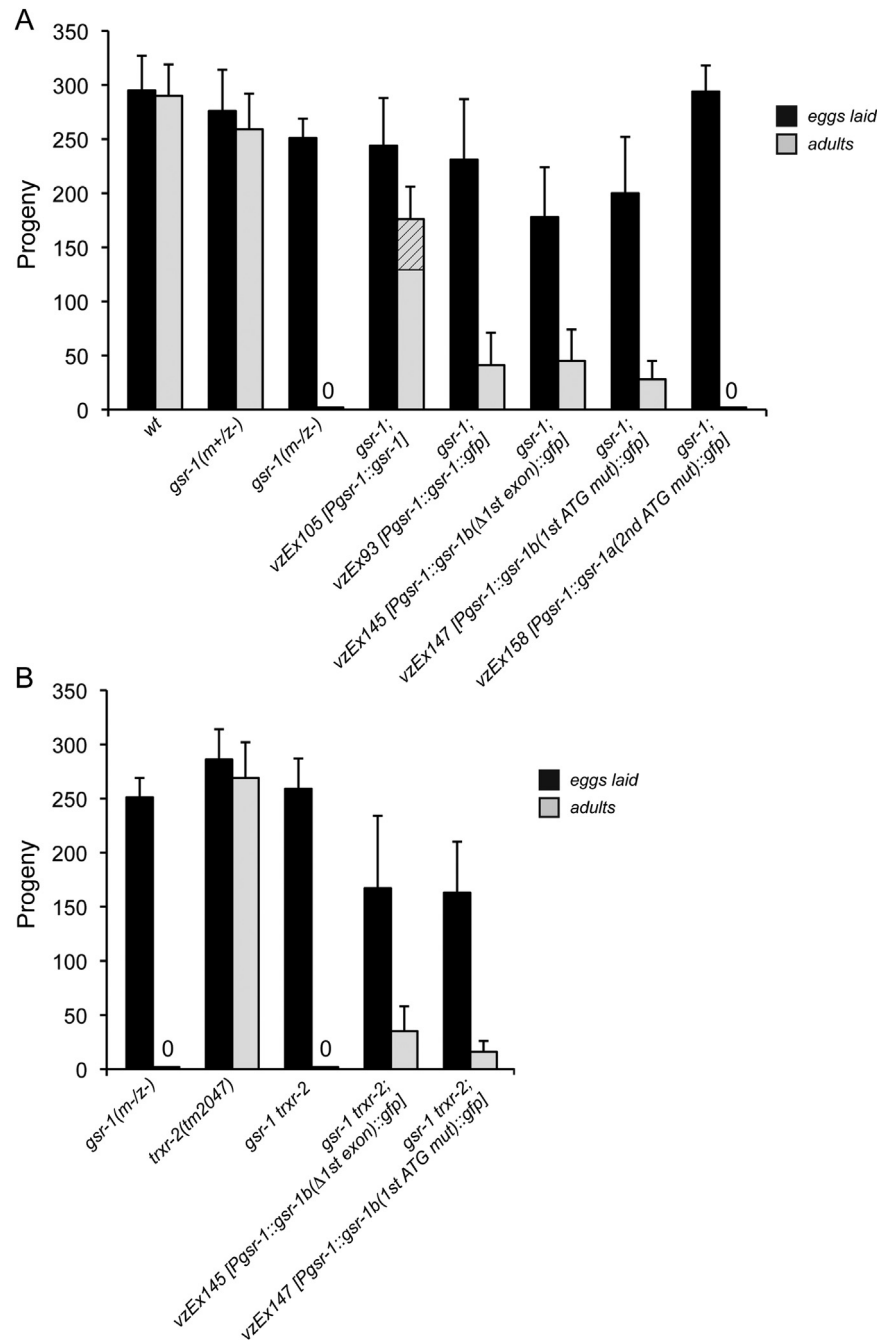


Fig. 7. Rescue of *gsr-1(tm3574)* mutants embryonic lethality. (A) The *gsr-1(tm3574)* embryonic lethal phenotype is rescued when GSR-1 activity is restored in the cytoplasm (GSR-1b, transgenes *vzEx145* and *vzEx147*) but not in mitochondria (GSR-1a, transgene *vzEx158*). The dashed bar in *gsr-1; vzEx105 [Pg_{gsr-1}::gsr-1]* animals indicates the fraction of viable, maternally rescued, non-transgenic progeny. Data are the mean \pm SD of the progeny from at least 10 animals of each genotype. (B) Viable progeny from *gsr-1; trxr-2* double mutant worms expressing GSR-1b::GFP in cytoplasm. Data are the mean \pm SD of the progeny from at least 10 animals of each genotype.

(*vzEx105* transgene) as well as GSR-1::GFP fusion protein (*vzEx93* transgene) (Fig. 7A), demonstrating that the lethality is due to a *gsr-1* deficiency. In contrast, no rescue was obtained when *gsr-1(m+,z-)* worms and their *gsr-1(m-,z-)* embryos were maintained on an effective external source of different GSH donors or precursors either in solid or liquid medium [5 mM GSH, 40 μ M S-linolenoyl-GSH [52]; 83 mg/ml liposomal GSH [53]; 20 μ M glutathione reduced ethyl ester [54]; 10 mM N-acetyl-L-cysteine [55]; 10 mM L-cystine, 10 mM L-methionine [56]) or 5 mM DTT (*data not shown*). This lack of rescue indicates that *gsr-1(m+,z-)* worms do not provide these compounds to their oocytes (or they are rapidly exhausted) and also reflects the inability of these chemicals to cross the *gsr-1(m-,z-)* embryo eggshell, which is non-permeable to most solutes [57].

As mentioned above, both wild type GSR-1 and GSR-1::GFP fusion protein rescue the *gsr-1* embryonic lethal phenotype. In *gsr-1; vzEx105 [Pgrr-1::gsr-1]* animals, untagged GSR-1 produced by the *vzEx105* transgene provides enough maternal load to allow the non-transgenic *gsr-1* progeny to reach the reproductive stage (Fig. 7A, dashed bar), similarly to *gsr-1(m+,z-)* worms segregating from *gsr-1/qC1* balanced parents. In contrast, in *gsr-1; vzEx93 [Pgrr-1::gsr-1::gfp]* animals, the GSR-1::GFP fusion protein produced by the *vzEx93* transgene fails to provide maternal rescue, so only the transgenic progeny carrying the *vzEx93* transgene are viable, while all the non-transgenic siblings arrest at early embryogenesis (difference between eggs laid and adults, Fig. 7A). The failure of the GSR-1::GFP fusion protein to provide maternal rescue could be explained by a lower enzymatic efficiency and/or a faster turnover of the GSR-1::GFP homodimers compared to wild type GSR-1 homodimers.

We next asked whether the embryonic lethal phenotype is due to a specific GSR-1 requirement in cytoplasm or mitochondria or, instead, to the simultaneous absence of the protein in both compartments. To address this, we performed isoform-specific rescue experiments in *gsr-1* mutants expressing, respectively, the mitochondrial GSR-1a::GFP or cytoplasmic GSR-1b::GFP fusion proteins (Fig. 2L–N). As GSR-1::GFP fusions do not provide maternal load, a qualitative determination of the isoform-specific rescue is possible by simply scoring viable vs non-viable progeny. Interestingly, while *gsr-1* mutants expressing GSR-1b::GFP exclusively in the cytoplasm (either from the *vzEx145 [Pgrr-1::gsr-1b(Δ 1st exon)::gfp]* or the *vzEx147 [Pgrr-1::gsr-1b(1st ATG mutated)::gfp]* transgenes) rescued the embryonic lethal phenotype, no viable progeny was obtained from *gsr-1* mutants expressing the mitochondrial specific GSR-1a::GFP isoform (from the *vzEx158 [Pgrr-1::gsr-1a(2nd ATG mutated)::gfp]* transgene) (Fig. 7A). These data imply that cytoplasmic GSR-1 is sufficient to restore normal embryonic development and that alternative redox systems such as the cytoplasmic thioredoxin system (redundant to the glutathione system in other organisms) are not able to substitute GSR-1 when absent from the cytoplasm.

The dispensability of mitochondrial GSR-1a, at least under non-stress normal growth conditions, could be explained by the presence of a redundant GSSG reducing system in mitochondria. In *S. cerevisiae* and *A. thaliana*, mitochondrial thioredoxin reductase is able to reduce GSSG in this organelle in the absence of mitochondrial glutathione reductase [58] (Meyer AJ, personal communication). To test if this genetic redundancy is maintained in *C. elegans*, we generated strains expressing only cytoplasmic GSR-1b::GFP (from *vzEx145* and *vzEx147* transgenes) in a *gsr-1(tm3574) trxr-2(tm2047)* double mutant background. As shown in Fig. 7B, restoring GSR-1 activity exclusively in the cytoplasm of *gsr-1 trxr-2* double mutants also produced viable progeny, arguing against TRXR-2 as a redundant system for mitochondrial GSR-1a in worms. Collectively, these data demonstrate that in *C. elegans*, cytoplasmic GSR-1b is essential for embryonic development and

that mitochondrial GSR-1a might be required for a yet to be identified dispensable function in this organelle.

3. Discussion

Most eukaryotic organisms have one single glutathione reductase gene encoding both cytoplasmic and mitochondrial isoforms by the use of alternative translation initiation sites [22–25]. In this study, we show that this is also the case for the *C. elegans* glutathione reductase *gsr-1* gene, where translation from the first ATG codon results in the mitochondrial GSR-1a isoform, with an N-terminal MTS mostly encoded by the first exon, while translation from a second in-frame ATG codon located at the beginning of the second exon generates the cytoplasmic isoform GSR-1b (Fig. 2L–T). Furthermore, *C. elegans* is one of the few examples of an eukaryotic organism with an essential requirement of glutathione reductase for viability. We show here that it is the cytoplasmic isoform of GSR-1 that is essential for viability (Fig. 7A). While in many organisms the thioredoxin system backups GSSG reduction in the absence of glutathione reductase [14] this appears not to be the case for *C. elegans*, despite the fact that both systems have been shown to cooperate in other processes such as worm molting [37]. Therefore, the *C. elegans* thioredoxin and glutathione systems share common functions but also have specific non-overlapping roles in worm physiology.

gsr-1 mutants with maternal load, *gsr-1(m+,z-)*, are viable and reach the reproductive stage indiscernibly from wild type controls. In turn, *gsr-1(m-,z-)* animals lacking maternal load arrest during early embryogenesis, displaying a robust progressive cell division delay phenotype (Fig. 6A) concomitant with an aberrant distribution of interphasic chromatin (Fig. 6B). Several possibilities might account for this lethal phenotype: i) as GSH depletion has been shown to inhibit DNA synthesis and to compromise cell cycle progression in mammalian cells [59,60], this dependence on GSH supply may also apply to *C. elegans* embryos. A possible mechanism could involve histone H3 glutathionylation that leads to a relaxed histone octamer in which DNA is less tightly packed around the nucleosome, thus opening chromatin [50]. Conversely, deglutathionylation of histone H3 results in a more compact distribution of chromatin ultimately decreasing gene expression and DNA synthesis. Thus, the absence of a GSH regenerating system in *gsr-1(m-,z-)* embryos could compromise nuclear histone H3 glutathionylation, which may explain the aberrant chromatin distribution and cell division delay; ii) related to the this, the thioredoxin and glutathione/glutaredoxin systems are the two enzymatic pathways providing reducing equivalents to the essential enzyme ribonucleotide reductase (RNR), responsible for the supply of deoxyribonucleotides for DNA synthesis and repair [61]. While the glutathione system is much more efficient with the *E. coli* RNR enzyme, in mammals the thioredoxin system is one order of magnitude more efficient than the glutaredoxin system [62]. If *C. elegans* RNR is more dependent on the glutathione system, as found in bacteria, failure to reduce RNR could be a cause of the lethality of *gsr-1(m-,z-)* worms; iii) mutations in mitochondrial genes have also been shown to cause embryonic arrest in *C. elegans* [47,48]. Although we have not been able to detect abnormal mitochondrial network distribution in *gsr-1(m-,z-)* embryos (Movie 4), the fact that maternally rescued *gsr-1* mutants have lower amount of mitochondria, increased mitochondrial fragmentation and induced levels of *hsp-6*, a mitochondrial stress reporter (Fig. 4), it is possible that impaired mitochondrial function may also account for the *gsr-1(m-,z-)* embryonic arrest phenotype; iv) alternatively, it is possible that *gsr-1(m-,z-)* embryos could die by GSSG poisoning. In mammalian cell cultures with compromised GSSG reducing activity, GSSG is excreted into the

cell culture medium to avoid the toxicity of its intracellular buildup [16]. If such mechanism also happens in *C. elegans gsr-1(m-,z-)* embryos, excreted GSSG would accumulate within the non-permeable extracellular peri-embryonic space of the embryo [63], where the progressive buildup of GSSG would ultimately cause embryo poisoning. It will be interesting to test this hypothesis by either microinjecting permeable GSH derivatives, GSH precursors or recombinant GSR-1 into the *gsr-1(m-,z-)* embryos [64] or by transgenically expressing GSR-1 in their peri-embryonic space.

As GSH synthesis is restricted to the cytoplasm, the mitochondrial GSH pool is generated by an active import of cytoplasmic GSH via specific carriers. In turn, it is generally accepted that mitochondrial GSSG is not readily exported from this organelle, being therefore reduced by mitochondrial glutathione reductase [65]. *C. elegans gsr-1* mutants with transgenic GSR-1 expression restricted to cytoplasm are viable, implying that mitochondrial glutathione reductase is dispensable in *C. elegans*, at least under normal non-stress conditions and, therefore, that GSSG does not accumulate in mitochondria. As mitochondrial thioredoxin reductase has been shown to substitute for mitochondrial glutathione reductase in yeast and plants [58] and (Meyer AJ, personal communication), we first tested whether this functional redundancy is maintained in *C. elegans*. However, a double mutant *gsr-1(m-,z-) trxr-2* (with transgenic GSR-1 expression in the cytoplasm to allow development) is also viable (Fig. 7B), suggesting that *trxr-2* is not functionally redundant with *gsr-1* in worms. We next asked whether mitochondrial GSR-1 is dispensable during normal non-stressed conditions but required under mitochondrial stresses to provide mitochondria with enough GSH to counteract the insults. We tested this possibility and demonstrate that animals lacking mitochondrial GSR-1 are as resistant as wild type controls when exposed to toxic doses of paraquat or juglone, thus ruling out that mitochondrial GSR-1 is needed under mitochondrial stress (Supplemental Fig. 2). In this context, the dispensability of mitochondrial *gsr-1* (and *trxr-2*) in *C. elegans* poses some interesting hypotheses: i) mitochondrial GSSG reduction is carried out by a third, yet unknown, mitochondrial reducing system in the absence of *gsr-1* and *trxr-2*; ii) GSSG can be exported from mitochondria to be reduced in the cytoplasm. Although studies in yeast show that the mitochondrial matrix and intermembrane space glutathione pools are maintained separately [66], a GSSG export activity has been described for the inner mitochondrial membrane ATP-binding cassette transporter ATM3 (in *A. thaliana*) and Atm1 (in *S. cerevisiae*) [67]. Thus, it is conceivable that GSSG generated in the mitochondrial matrix could be exported to the intermembrane space by these transporters, from where it can reach the cytoplasm via porins [66] to be reduced by cytoplasmic glutathione reductase as there is no GSSG reducing system in the mitochondrial intermembrane space. The *C. elegans abtm-1* gene is the ortholog of ATM3/Atm1 and its mutation causes embryonic lethality. Instead, worms with downregulated levels of *abtm-1* by RNAi are viable, although have increased oxidative stress and ferric iron accumulation [68]. This lethality of *abtm-1* mutants is presumably originated by a failure to transport Fe-S clusters to cytoplasm rather than a GSSG accumulation in mitochondria, as these animals are wild type for *gsr-1*. We performed *abtm-1* RNAi in *gsr-1(m+,z-)* worms and did not observe any compound phenotype, suggesting that GSSG is not accumulating in their mitochondria, even in the absence of this putative GSSG exporter (*data now shown*); iii) alternatively, mitochondrial GSR-1 could be needed for yet unknown additional non-essential roles in this organelle, other than reducing GSSG. An example of a novel additional function of glutathione reductase is the reduction of the redox-regulated mitoNEET protein, an outer mitochondrial membrane protein that has been implicated in energy homeostasis and mitophagy [69,70].

In summary, we describe here the phenotypes that the absence of glutathione reductase causes in the model organism *C. elegans*. The availability of cytoplasmic and mitochondrial thioredoxin reductase mutants in this organism, and the fact that *gsr-1* has now been characterised, offers an ideal scenario where to study the respective contribution of the different compartmentalized redox systems in the context of a multicellular organism. Although our results clearly show that GSR-1 is dispensable in mitochondria, it is yet intriguing why *gsr-1(m+,z-)* mutants display mitochondria-associated phenotypes. It is plausible that under limiting GSR-1 availability as in *gsr-1(m+,z-)* mutants, resources are derived to maintain the essential cytoplasmic function thus provoking mitochondrial susceptibility. Future studies aimed to specifically inactivate *gsr-1* mitochondrial or cytoplasmic isoforms by CRISPR technology will be instrumental to further refine their respective contribution to cell function and redox homeostasis.

4. Materials and methods

4.1. *C. elegans* strains and culture conditions

The standard methods used for culturing and maintenance of *C. elegans* were as previously described [71]. The strains used in this work are described in Supplemental Table 1. All experiments were performed at 20 °C unless otherwise noted. All VZ strains are 6x backcrossed with N2 wild type.

4.2. *gsr-1* expression constructs, transgenesis and image analysis of transgenic animals

For fluorescent reporter constructs, DNA fragments containing the 2.2 kb upstream promoter region of the *gsr-1* gene (including the first 15 nucleotides of the coding region), the 2.2 kb promoter region plus the complete *gsr-1* genomic ORF and the *gsr-1* genomic ORF except the first exon were amplified from *C. elegans* wild type genomic DNA and cloned into the PstI and Ball sites of the pPD95.81 vector (Fire Lab *C. elegans* Vector Kit 1995 (unpublished)) to generate *gsr-1* transcriptional and translational GFP reporters, respectively. Mutagenesis reactions (1st exon deletion and 1st and 2nd ATG codon substitutions) were performed on the 2.2 kb promoter *gsr-1* translational GFP reporter construct using the QuickChange II XL Site Directed Mutagenesis Kit (Stratagene) and confirmed by sequencing. For the reporter construct targeting GFP to muscle cell mitochondria directed by *gsr-1* MTS, we amplified a 2.4 kb region of the *myo-3* gene promoter with primers that included the *gsr-1* MTS sequence from the pBN42 plasmid ([*Pmyo-3::gfp::3'-UTRunc-54*] [72]) and cloned it into the BamHI site of the pPD95.81 vector. Correct orientation of the insert was confirmed by sequencing. For expression of wild type GSR-1, we amplified a fragment containing the *gsr-1* 2.2 kb promoter region, the genomic ORF and 3'-UTR from *C. elegans* wild type genomic DNA and cloned it into the PstI and SpeI sites of the pSPARK I vector (Canvax Biotech). The sequences of all primers used for cloning are available upon request. Transgenic worms were generated by DNA microinjection as previously described [73]. The pRF4 [*rol-6(su1006)*] [73] and coel::GFP [*Punc-122::gfp*] [74] plasmids were used as coinjection markers at 50 ng/μl. The *gsr-1* expression constructs described above were injected into N2 wild type animals (either as circular plasmids or linear fragments) at varying concentrations ranging from 10 to 50 ng/μl.

For image analysis of fluorescent transgenic worms, animals were mounted in a 5 μl drop of 10 mM levamisole on a 3% agarose pad covered with a coverslip. Differential interference contrast (DIC) and fluorescence imaging was performed on a Zeiss Axio-Imager M2 with ApoTome Unit fluorescence microscope and

images were captured with the AxioVision 4.8 Software (Zeiss) (Fig. 2A–K).

4.3. Imaging of mitochondria, sarcomeres and measures of mitochondrial function

For Figs. 2M–N and 2R–T, animals were picked into 25 ml M9 buffer and were immobilized only by the pressure from the cover slip. Images in M and N were taken using a Nikon H600L microscope (Nikon Corporation, Tokyo, Japan) and a Nikon Digital Sight DS-Fi1 digital camera with proprietary software. Images R – T were taken on a Zeiss AX10 microscope (Carl Zeiss AG, Oberkochen, Germany) with an Axiocam MRC digital camera and Axiovision LE software. Images R – T were taken using GFP, RFP, and triple-pass filter sets, respectively. Images in Fig. 4A were taken in $n=60$ animals and 4B–C in $n=20$ animals at young adulthood. Images in 4C were taken with a fixed exposure of 1 s and the fluorescence was quantified using ImageJ. Corrected total animal fluorescence was calculated using data from integrated density and area, however, mean fluorescence minus background fluorescence produced a similar result. Data were non-parametric and were therefore analysed using a Mann Whitney test and significance was set at $p < 0.05$.

4.4. RNA extraction and RT-PCR

For total RNA extraction, gravid hermaphrodites were washed off the plates with M9 buffer and dissolved in 5 M NaOH bleaching solution. Embryos were collected and washed several times with M9 buffer. RNA was extracted from embryos using the NucleoSpin RNA II (Macherey-Nagel) kit following the manufacturer's instructions. Total RNA was DNase-treated using the Amplification Grade Dnase I (Sigma) and 1 μ g of Dnase-treated RNA was reverse transcribed in a 20 μ l reaction mixture. cDNA was generated using the iScript™ cDNA Synthesis Kit (Biorad). 1 μ g of cDNA was used for *gsr-1* RT-PCR reactions using MBL-Taq DNA Polymerase (Dominion-MBL).

4.5. Recombinant protein expression, purification and glutathione reductase enzymatic activity

gsr-1 cDNA from N2 wild type and *gsr-1(tm3574)* mutants was amplified with the forward primer 5'-ACTGCATATGCTGGCGTCAAG-3' and the reverse primer 5'-CATGCTCGAGTTATTATCCGGCTTCACAC-3' and cloned into the NdeI and XhoI restriction sites of the pET-15b vector (Novagen) to generate the constructs His-GSR-1b and His- Δ GSR-1b, respectively. These constructs were used to transform the *E. coli* BL21(DE3) strain and recombinant protein expression was induced by adding 0.5 mM IPTG to a 500 ml LB medium bacteria culture of 0.5–0.7 OD supplemented with 0.1 mg/ml ampicillin and further incubating the cells at 25 °C and 200 rpm during 5 h. Cells were collected by centrifugation, immediately resuspended in 25 ml Tris–HCl 20 mM pH 8, 0.1 M NaCl buffer supplemented with 15 mg de lysozyme and 30 mg de Dnase I. After 5 min incubation at room temperature the preparation was sonicated for 30 min on ice and the cell free extract was obtained by centrifugation at 10,000g during 30 min at 4 °C. Recombinant His-GSR-1b and His- Δ GSR-1b proteins were purified from the cell free extract using a TALON column (Clontech) equilibrated with Tris–HCl 20 mM pH 8, 0.1 M NaCl buffer and eluted with 100 mM imidazol. Finally, the purified proteins were dialyzed against the same buffer and concentrated using Centricon YM-10 filter devices (Millipore). The glutathione reductase enzymatic activity was determined as previously described [75]. Briefly, a standard assay mixture (0.5 ml) containing potassium phosphate buffer 0.1 M, pH 7.2, EDTA 1 mM, NADPH

200 μ M, with different concentrations of His-GSR-1b and His- Δ GSR-1b was prepared and the reaction was initiated by addition of 0.5 mM GSSG. The decrease of absorbance at 340 nm (indicating NADPH consumption) was recorded spectrophotometrically at 25 °C.

4.6. Embryonic cell lineage analysis

For embryonic cell lineage analysis, 4D-microscopy was carried out using standard live-animal mounting techniques on a Leica DM6000 microscope fitted with DIC optics. The use of DIC optics allows cells tracing without using any dye or fluorescent marker that might alter the cell cycle progression. Embryonic cell lineage was determined as described [76]. In summary, gravid hermaphrodites were dissected and 2-to 4-cell stage embryos were mounted on 4% agar pads in water, and sealed with Vaseline. Imaging was performed at 25 °C. The multi-focal time-lapse microscopy of the samples was controlled with the open source software Micro-manager (www.micro-manager.org). Pictures on 30 focal planes (1 μ m/section) were taken every 30 s for 12 h. Embryo lineages were analyzed with the software SimiBiocel (SIMI GmbH, www.simi.com).

4.7. Brood size determination

L4 larvae were singled onto OP50 seeded plates, allowed to lay eggs at 20 °C and transferred to new plates every 12 h until the animals stopped reproducing. Eggs were counted and then incubated further at 20 °C to quantify adult progeny four days later.

4.8. Longevity assay

Lifespan assays were performed at 20 °C as previously described [77] with slight modifications. Tightly synchronized embryos from gravid adult hermaphrodites were allowed to develop through the L4 larval stage and then transferred to fresh NGM plates in groups of 20 worms per plate for a total of 80 individuals per experiment. The day animals reached the L4 larval stage was used as $t=0$. Animals were transferred to fresh plates daily until progeny production ceased and after that they were transferred every second to third day but monitored daily for dead animals. Nematodes that did not respond to gentle prodding and displayed no pharyngeal pumping were scored as dead. Animals that crawled off the plate or died due to internal hatching or extruded gonad were censored and incorporated as such into the data set.

4.9. Paraquat and Juglone acute treatment

Plates containing the appropriate amount of the respective chemical were prepared freshly prior the experiment. To minimize the number of animals crawling off the agar, OP50 bacteria (from seeded plates) was directly spread in the center of the plates using an inoculating loop. L4 larvae were transferred to plates and survival was determined after 16 h incubation at 20 °C. Nematodes that did not respond to gentle prodding and displayed no pharyngeal pumping were scored as dead. Animals that crawled off the plate were censored.

4.10. Embryonic/larval arrest assays

10 gravid *trx-1(sv47); gsr-1(tm3574)/qC1::rfp* hermaphrodites were allowed to lay eggs during 3 h at 20 °C and subsequently removed. Embryos were counted and then allowed to develop for 4 days at 20 °C after which non RFP *trx-1(sv47); gsr-1(m+,z-)* adults, larvae and unhatched embryos were quantified.

4.11. SKN-1 dependent gene expression quantification and nuclear translocation of SKN-1 fluorescent reporter

Worms at their third day of adulthood expressing *dvEx166* [*Pgst-4::gfp*] and *svEx741* [*Pgcs-1::gfp*] extrachromosomal arrays were mounted in a 5 ml drop of 10 mM levamisole on a 3% agarose pad covered with a coverslip. Fluorescence imaging was performed on a Olympus BX61 fluorescence microscope equipped with a Olympus DP72 camera and images were captured with the CellSensDimension 1.12 Software (Olympus). All micrographs were taken with identical image capture settings and quantification of GFP expression (measured as the fluorescence mean of 25 worms divided by the selected area and normalized by the background adjacent to the selected worm in the same image) was performed using the ImageJ Software (NIH). When needed, equal adjustment of brightness and contrast on control and matched problem images was implemented using Adobe Photoshop 10 Software (Adobe Systems). To visualize SKN-1B/C::GFP nuclear translocation, young adults were washed from plates, anesthetized with 1 mM levamisole and mounted on 2% agarose pads. Visualization and imaging was performed using an Olympus IX81 automated inverted microscope and Slidebook (version 5.0) software. SKN-1B/C::GFP localization quantification, the percent intestinal SKN-1 nuclear localization was categorically scored as follows: none: no localization, low: posterior or anterior intestinal localization, medium: posterior and anterior intestinal localization, high: localization throughout the entire intestine [78].

4.12. Mitochondrial related phenotypes

To determine if *gsr-1* deficiency had any effect on mitochondria related phenotypes, age-synchronized, young adult animals ($n=60$) were assessed for mitochondrial networking in *gsr-1(m+,z-); ccls4251* [*Pmyo-3::mito::gfp*] vs control *ccls4251* [*Pmyo-3::mito::gfp*] animals. There was significantly greater mitochondrial fragmentation in the *gsr-1* animals than controls at 20 °C ($p < 0.001$) and 25 °C ($p < 0.05$). Determination of sarcomere structure in *gsr-1(m+,z-); jls01* [*Pmyo-3::myo-3::gfp*] were compared to control *jls01* [*Pmyo-3::myo-3::gfp*] animals ($n=20$ per group) both at 20 °C and at 25 °C. There was no significant difference between groups ($p > 0.05$). For mitochondrial content determination, we loaded animals with JC-10, a dye that accumulates proportionally to a negative mitochondrial membrane potential as previously described [79]. Wild type control animals had significantly greater fluorescence of the gut mitochondria than did *gsr-1(m+,z-)* animals ($p < 0.001$). Images were taken with a fixed exposure of 1 s on the Nikon H600L microscope and the fluorescence was quantified using ImageJ. Corrected total animal fluorescence was calculated as follows: Integrated density – area of the worm \times mean fluorescence of three background readings. Data were analyzed using a Mann-Whitney test as data were non-parametric.

4.13. Embryonic chromatin dynamics analysis

BN323 animals were maintained at 16 °C and shifted to 25 °C 2 h prior to microscopy. Heterozygous and homozygous *gsr-1* mutants were dissected and early embryos were mounted together in M9 buffer on 2% agarose pads. Coverslips were placed over the embryos and sealed with VALAP (1:1:1 mixture of Vaseline, lanolin and paraffin). Confocal epifluorescence and DIC images from three focal planes were acquired at 25 °C every 10 min on a Nikon A1R microscope through a Plan Apo VC 60x/1.4 objective (Nikon, Tokyo, Japan) using a pinhole of 39.7 μ m (1.2 Airy Units).

Acknowledgments

Some strains were provided by the CGC, which is funded by NIH Office of Research Infrastructure Programs (P40 OD010440) and by the Japanese National Bioresource Project. We thank Cristina Cecchi, Amir Shapir, Paul Sternberg, Bart Braeckman, Chris Link, Simon Tuck, Keith Blackwell, José López-Barneo and LivOn Labs for strains and chemicals, Katie McCallum and Danielle Garsin for their help with *skn-1* experiments and Elizabeth Veal and Michel Toledano for critical reading of the manuscript. Prof. Rafael Fernández-Chacón is deeply acknowledged for his continuous support. AMV was supported by grants from the Spanish Ministry of Economy and Competitiveness (BFU2015-64408-P) and the Instituto de Salud Carlos III (PI11/00072, cofinanced by the Fondo Social Europeo) and is a member of the GENIE and EU-ROS Cost Action of the European Union. NJS was supported by a grant from the US National Institutes of Health National Institute for Arthritis and Musculoskeletal and Skin Diseases (AR-054342). CJG was funded by a Doctoral Training Studentship provided by the University of Nottingham. PA was supported by the Spanish Ministry of Economy and Competitiveness (BFU2013-42709P). JC is a member of the GENIE Cost action and was funded by Rioja Salud Foundation (Onco-2-2015).

Appendix A. Supplementary Information

Supplementary data associated with this article can be found in the online version at <http://dx.doi.org/10.1016/j.freeradbiomed.2016.04.017>.

References

- [1] E.M. Hanschmann, J.R. Godoy, C. Berndt, C. Hudemann, C.H. Lillig, Thioredoxins, glutaredoxins, and peroxiredoxins—molecular mechanisms and health significance: from cofactors to antioxidants to redox signaling, *Antioxid. Redox Signal.* 19 (2013) 1539–1605.
- [2] Y. Meyer, B.B. Buchanan, F. Vignols, J.P. Reichheld, Thioredoxins and glutaredoxins: unifying elements in redox biology, *Annu. Rev. Genet.* 43 (2009) 335–367.
- [3] Y. Xiong, J.D. Uys, K.D. Tew, D.M. Townsend, S-glutathionylation: from molecular mechanisms to health outcomes, *Antioxid. Redox Signal.* 15 (2011) 233–270.
- [4] R.C. Fahey, A.R. Sundquist, Evolution of glutathione metabolism, *Adv. Enzymol. Relat. Areas Mol. Biol.* 64 (1991) 1–53.
- [5] C.M. Grant, F.H. MacIver, I.W. Dawes, Glutathione is an essential metabolite required for resistance to oxidative stress in the yeast *Saccharomyces cerevisiae*, *Curr. Genet.* 29 (1996) 511–515.
- [6] C. Romero-Aristizabal, D.S. Marks, W. Fontana, J. Apfeld, Regulated spatial organization and sensitivity of cytosolic protein oxidation in *Caenorhabditis elegans*, *Nat. Commun.* 5 (2014) 5020.
- [7] J.A. Fraser, P. Kansagra, C. Kotecki, R.D. Saunders, L.I. McLellan, The modifier subunit of *Drosophila* glutamate-cysteine ligase regulates catalytic activity by covalent and noncovalent interactions and influences glutathione homeostasis in vivo, *J. Biol. Chem.* 278 (2003) 46369–46377.
- [8] N.G. Cairns, M. Pasternak, A. Wachter, C.S. Cobbett, A.J. Meyer, Maturation of arabidopsis seeds is dependent on glutathione biosynthesis within the embryo, *Plant Physiol.* 141 (2006) 446–455.
- [9] T.P. Dalton, M.Z. Dieter, Y. Yang, H.G. Shertzer, D.W. Nebert, Knockout of the mouse glutamate cysteine ligase catalytic subunit (Gclc) gene: embryonic lethal when homozygous, and proposed model for moderate glutathione deficiency when heterozygous, *Biochem. Biophys. Res. Commun.* 279 (2000) 324–329.
- [10] M. Pasternak, B. Lim, M. Wirtz, R. Hell, C.S. Cobbett, A.J. Meyer, Restricting glutathione biosynthesis to the cytosol is sufficient for normal plant development, *Plant J.* 53 (2008) 999–1012.
- [11] A. Winkler, R. Njalsson, K. Carlsson, A. Elgadi, B. Rozell, L. Abraham, N. Ercal, Z. Shi, M.W. Lieberman, A. Larsson, S. Norgren, Glutathione is essential for early embryogenesis—analysis of a glutathione synthetase knockout mouse, *Biochem. Biophys. Res. Commun.* 412 (2011) 121–126.
- [12] C.M. Grant, F.H. MacIver, I.W. Dawes, Glutathione synthetase is dispensable for growth under both normal and oxidative stress conditions in the yeast *Saccharomyces cerevisiae* due to an accumulation of the dipeptide gamma-glutamylcysteine, *Mol. Biol. Cell* 8 (1997) 1699–1707.

- [13] T. Logan-Garbisch, A. Bortolazzo, P. Luu, A. Ford, D. Do, P. Khodabakhshi, R. L. French, Developmental ethanol exposure leads to dysregulation of lipid metabolism and oxidative stress in *Drosophila*, *G3* 5 (2014) 49–59.
- [14] S.M. Kanzok, R.H. Schirmer, I. Turbachova, R. Jozef, K. Becker, The thioredoxin system of the malaria parasite *Plasmodium falciparum*. Glutathione reduction revisited, *J. Biol. Chem.* 275 (2000) 40180–40186.
- [15] B. Morgan, D. Ezerina, T.N. Amoako, J. Riemer, M. Seedorf, T.P. Dick, Multiple glutathione disulfide removal pathways mediate cytosolic redox homeostasis, *Nat. Chem. Biol.* 9 (2013) 119–125.
- [16] S. Eriksson, J.R. Prigge, E.A. Talago, E.S. Arner, E.E. Schmidt, Dietary methionine can sustain cytosolic redox homeostasis in the mouse liver, *Nat. Commun.* 6 (2015) 6479.
- [17] J. Lee, I.W. Dawes, J.H. Roe, Isolation, expression, and regulation of the *pgr1*(+) gene encoding glutathione reductase absolutely required for the growth of *Schizosaccharomyces pombe*, *J. Biol. Chem.* 272 (1997) 23042–23049.
- [18] R. Pastrana-Mena, R.R. Dinglasan, B. Franke-Fayard, J. Vega-Rodriguez, M. Fuentes-Caraballo, A. Baerga-Ortiz, I. Coppens, M. Jacobs-Lorena, C.J. Janse, A.E. Serrano, Glutathione reductase-null malaria parasites have normal blood stage growth but arrest during development in the mosquito, *J. Biol. Chem.* 285 (2010) 27045–27056.
- [19] I. Tzafrir, R. Pena-Muralla, A. Dickerman, M. Berg, R. Rogers, S. Hutchens, T. C. Sweeney, J. McElver, G. Aux, D. Patton, D. Meinke, Identification of genes required for embryo development in *Arabidopsis*, *Plant Physiol.* 135 (2004) 1206–1220.
- [20] S.M. Kanzok, A. Fechner, H. Bauer, J.K. Ulschmid, H.M. Muller, J. Botella-Munoz, S. Schneuwly, R. Schirmer, K. Becker, Substitution of the thioredoxin system for glutathione reductase in *Drosophila melanogaster*, *Science* 291 (2001) 643–646.
- [21] Y. Meyer, C. Belin, V. Delorme-Hinoux, J.P. Reichheld, C. Riondet, Thioredoxin and glutaredoxin systems in plants: molecular mechanisms, cross talks and functional significance, *Antioxid. Redox Signal.* 17 (2012) 1124–1160.
- [22] M.J. Kelner, M.A. Montoya, Structural organization of the human glutathione reductase gene: determination of correct cDNA sequence and identification of a mitochondrial leader sequence, *Biochem. Biophys. Res. Commun.* 269 (2000) 366–368.
- [23] T. Tamura, H.W. McMicken, C.V. Smith, T.N. Hansen, Gene structure for mouse glutathione reductase, including a putative mitochondrial targeting signal, *Biochem. Biophys. Res. Commun.* 237 (1997) 419–422.
- [24] C.E. Outten, V.C. Culotta, Alternative start sites in the *Saccharomyces cerevisiae* GLR1 gene are responsible for mitochondrial and cytosolic isoforms of glutathione reductase, *J. Biol. Chem.* 279 (2004) 7785–7791.
- [25] J.Y. Song, J. Cha, J. Lee, J.H. Roe, Glutathione reductase and a mitochondrial thioredoxin play overlapping roles in maintaining iron-sulfur enzymes in fission yeast, *Eukaryot. Cell* 5 (2006) 1857–1865.
- [26] W.A. Prinz, F. Aslund, A. Holmgren, J. Beckwith, The role of the thioredoxin and glutaredoxin pathways in reducing protein disulfide bonds in the *Escherichia coli* cytoplasm, *J. Biol. Chem.* 272 (1997) 15661–15667.
- [27] C. Kumar, A. Igbaria, B. D'Autreaux, A.G. Planson, C. Junot, E. Godat, A. K. Bachhawat, A. Delaunay-Moisán, M.B. Toledano, Glutathione revisited: a vital function in iron metabolism and ancillary role in thiol-redox control, *EMBO J.* 30 (2011) 2044–2056.
- [28] M.B. Toledano, A. Delaunay-Moisán, C.E. Outten, A. Igbaria, Functions and cellular compartmentation of the thioredoxin and glutathione pathways in yeast, *Antioxid. Redox Signal.* 18 (2013) 1699–1711.
- [29] I. Gostimskaya, C.M. Grant, Yeast mitochondrial glutathione is an essential antioxidant with mitochondrial thioredoxin providing a back-up system, *Free Radic. Biol. Med.* 94 (2016) 55–65.
- [30] L.K. Rogers, T. Tamura, B.J. Rogers, S.E. Welty, T.N. Hansen, C.V. Smith, Analyses of glutathione reductase hypomorphic mice indicate a genetic knockout, *Toxicol. Sci.* 82 (2004) 367–373.
- [31] M. Matsui, M. Oshima, H. Oshima, K. Takaku, T. Maruyama, J. Yodoi, M. M. Taketo, Early embryonic lethality caused by targeted disruption of the mouse thioredoxin gene, *Dev. Biol.* 178 (1996) 179–185.
- [32] M. Conrad, C. Jakupoglu, S.G. Moreno, S. Lipp, A. Banjac, M. Schneider, H. Beck, A.K. Hatzopoulos, U. Just, F. Sinowatz, W. Schmahl, K.R. Chien, W. Wurst, G. W. Bornkamm, M. Brielmeier, Essential role for mitochondrial thioredoxin reductase in hematopoiesis, heart development, and heart function, *Mol. Cell. Biol.* 24 (2004) 9414–9423.
- [33] C. Jakupoglu, G.K. Przemeck, M. Schneider, S.G. Moreno, N. Mayr, A. K. Hatzopoulos, M.H. de Angelis, W. Wurst, G.W. Bornkamm, M. Brielmeier, M. Conrad, Cytoplasmic thioredoxin reductase is essential for embryogenesis but dispensable for cardiac development, *Mol. Cell. Biol.* 25 (2005) 1980–1988.
- [34] L. Nonn, R.R. Williams, R.P. Erickson, G. Powis, The absence of mitochondrial thioredoxin 2 causes massive apoptosis, exencephaly, and early embryonic lethality in homozygous mice, *Mol. Cell. Biol.* 23 (2003) 916–922.
- [35] P.K. Mandal, M. Schneider, P. Kolle, P. Kuhlencordt, H. Forster, H. Beck, G. W. Bornkamm, M. Conrad, Loss of thioredoxin reductase 1 renders tumors highly susceptible to pharmacologic glutathione deprivation, *Cancer Res.* 70 (2010) 9505–9514.
- [36] E.S. Suvorova, O. Lucas, C.M. Weisend, M.F. Rollins, G.F. Merrill, M.R. Capecchi, E.E. Schmidt, Cytoprotective Nrf2 pathway is induced in chronically *txnr1*-deficient hepatocytes, *PLoS One* 4 (2009) e6158.
- [37] J. Stenvall, J.C. Fierro-Gonzalez, P. Swoboda, K. Saamarthy, Q. Cheng, B. Cacho-Valadez, E.S. Arner, O.P. Persson, A. Miranda-Vizuete, S. Tuck, Selenoprotein TRXR-1 and GSR-1 are essential for removal of old cuticle during molting in *Caenorhabditis elegans*, *Proc. Natl. Acad. Sci. USA* 108 (2011) 1064–1069.
- [38] B. Cacho-Valadez, F. Munoz-Lobato, J.R. Pedrajas, J. Cabello, J.C. Fierro-Gonzalez, P. Navas, P. Swoboda, C.D. Link, A. Miranda-Vizuete, The characterization of the *Caenorhabditis elegans* mitochondrial thioredoxin system uncovers an unexpected protective role of thioredoxin reductase 2 in beta-amyloid peptide toxicity, *Antioxid. Redox Signal.* 16 (2012) 1384–1400.
- [39] K. Luersen, D. Stegehake, J. Daniel, M. Drescher, I. Ajonina, C. Ajonina, P. Hertel, C. Woltersdorf, E. Liebau, The glutathione reductase GSR-1 determines stress tolerance and longevity in *Caenorhabditis elegans*, *PLoS One* 8 (2013) e60731.
- [40] S.J. Habib, W. Neupert, D. Rapaport, Analysis and prediction of mitochondrial targeting signals, *Methods Cell Biol.* 80 (2007) 761–781.
- [41] J.P. Hendrick, P.E. Hodges, L.E. Rosenberg, Survey of amino-terminal proteolytic cleavage sites in mitochondrial precursor proteins: leader peptides cleaved by two matrix proteases share a three-amino acid motif, *Proc. Natl. Acad. Sci. USA* 86 (1989) 4056–4060.
- [42] J.I. Fuxman Bass, A.M. Tamburino, A. Mori, N. Beittel, M.T. Weirauch, J.S. Reece-Hoyes, A.J. Walhout, Transcription factor binding to *Caenorhabditis elegans* first introns reveals lack of redundancy with gene promoters, *Nucleic Acids Res.* 42 (2014) 153–162.
- [43] E. Petit, X. Michelet, C. Rauch, J. Bertrand-Michel, F. Terce, R. Legouis, F. Morel, Glutathione transferases kappa 1 and kappa 2 localize in peroxisomes and mitochondria, respectively, and are involved in lipid metabolism and respiration in *Caenorhabditis elegans*, *FEBS J.* 276 (2009) 5030–5040.
- [44] M.L. Edgley, D.L. Baillie, D.L. Riddle, A.M. Rose, Genetic balancers, *WormBook* (2006) 1–32.
- [45] J. Wang, S. Robida-Stubbs, J.M. Tullet, J.F. Rual, M. Vidal, T.K. Blackwell, RNAi screening implicates a SKN-1-dependent transcriptional response in stress resistance and longevity deriving from translation inhibition, *PLoS Genet.* 8 (2010) e1001048.
- [46] T. Yoneda, C. Benedetti, F. Urano, S.G. Clark, H.P. Harding, D. Ron, Compartment-specific perturbation of protein handling activates genes encoding mitochondrial chaperones, *J. Cell Sci.* 117 (2004) 4055–4066.
- [47] J. Ahninger, Embryonic tissue differentiation in *Caenorhabditis elegans* requires *dif-1*, a gene homologous to mitochondrial solute carriers, *EMBO J.* 14 (1995) 2307–2316.
- [48] C. Asencio, P. Navas, J. Cabello, R. Schnabel, J.R. Cypser, T.E. Johnson, J. C. Rodriguez-Aguilera, Coenzyme Q supports distinct developmental processes in *Caenorhabditis elegans*, *Mech. Ageing Dev.* 130 (2009) 145–153.
- [49] A.V. Kruger, R. Jelier, O. Dzyubachyk, T. Zimmermann, E. Meijering, B. Lehner, Comprehensive single cell-resolution analysis of the role of chromatin regulators in early *C. elegans* embryogenesis, *Dev. Biol.* 398 (2015) 153–162.
- [50] J.L. Garcia-Gimenez, G. Olaso, S.B. Hake, C. Bonisch, S.M. Wiedemann, J. Markovic, F. Dasi, A. Gimeno, C. Perez-Quilis, O. Palacios, M. Capdevila, J. Vina, F.V. Pallardo, Histone h3 glutathionylation in proliferating mammalian cells destabilizes nucleosomal structure, *Antioxid. Redox Signal.* 19 (2013) 1305–1320.
- [51] A.S. Badrinath, J.G. White, Contrasting patterns of mitochondrial redistribution in the early lineages of *Caenorhabditis elegans* and *Acroboloides* sp. PS1146, *Dev. Biol.* 258 (2003) 70–75.
- [52] R. Cascella, E. Evangelisti, M. Zampagni, M. Becatti, G. D'Adamo, A. Goti, G. Liguri, C. Fiorillo, C. Cecchi, S-linolenoyl glutathione intake extends lifespan and stress resistance via Sir-2.1 upregulation in *Caenorhabditis elegans*, *Free Radic. Biol. Med.* 73 (2014) 127–135.
- [53] A. Shibamura, T. Ikeda, Y. Nishikawa, A method for oral administration of hydrophilic substances to *Caenorhabditis elegans*: effects of oral supplementation with antioxidants on the nematode lifespan, *Mech. Ageing Dev.* 130 (2009) 652–655.
- [54] E.J. Levy, M.E. Anderson, A. Meister, Transport of glutathione diethyl ester into human cells, *Proc. Natl. Acad. Sci. USA* 90 (1993) 9171–9175.
- [55] W. Yang, S. Hekimi, A mitochondrial superoxide signal triggers increased longevity in *Caenorhabditis elegans*, *PLoS Biol.* 8 (2010) e1000556.
- [56] C. Edwards, J. Canfield, N. Copes, A. Brito, M. Rehan, D. Lipps, J. Brunquell, S. D. Westerheide, P.C. Bradshaw, Mechanisms of amino acid-mediated lifespan extension in *Caenorhabditis elegans*, *BMC Genet.* 16 (2015) 8.
- [57] D. Wharton, Nematode egg-shells, *Parasitology* 81 (1980) 447–463.
- [58] E.W. Trotter, C.M. Grant, Overlapping roles of the cytoplasmic and mitochondrial redox regulatory systems in the yeast *Saccharomyces cerevisiae*, *Eukaryot. Cell* 4 (2005) 392–400.
- [59] L.A. Dethlefsen, C.M. Lehman, J.E. Biaglow, V.M. Peck, Toxic effects of acute glutathione depletion by buthionine sulfoximine and dimethylfumarate on murine mammary carcinoma cells, *Radiat. Res.* 114 (1988) 215–224.
- [60] J. Markovic, N.J. Mora, A.M. Broseta, A. Gimeno, N. de-la-Concepcion, J. Vina, F. V. Pallardo, The depletion of nuclear glutathione impairs cell proliferation in 3T3 fibroblasts, *PLoS One* 4 (2009) e6413.
- [61] R. Sengupta, A. Holmgren, Thioredoxin and glutaredoxin-mediated redox regulation of ribonucleotide reductase, *World J. Biol. Chem.* 5 (2014) 68–74.
- [62] F. Zahedi Avval, A. Holmgren, Molecular mechanisms of thioredoxin and glutaredoxin as hydrogen donors for Mammalian s phase ribonucleotide reductase, *J. Biol. Chem.* 284 (2009) 8233–8240.
- [63] S.K. Olson, G. Greenan, A. Desai, T. Muller-Reichert, K. Oegema, Hierarchical assembly of the eggshell and permeability barrier in *C. elegans*, *J. Cell Biol.* 198 (2012) 731–748.
- [64] L.D. Brennan, T. Roland, D.G. Morton, S.M. Fellman, S. Chung, M. Soltani, J. W. Kevek, P.M. McEuen, K.J. Kempfues, M.D. Wang, Small molecule injection into single-cell *C. elegans* embryos via carbon-reinforced nanopipettes, *PLoS One* 8 (2013) e75712.
- [65] V. Ribas, C. Garcia-Ruiz, J.C. Fernandez-Checa, Glutathione and mitochondria,

- Front. Pharmacol. 5 (2014) 151.
- [66] K. Kojer, M. Bien, H. Gangel, B. Morgan, T.P. Dick, J. Riemer, Glutathione redox potential in the mitochondrial intermembrane space is linked to the cytosol and impacts the Mia40 redox state, *EMBO J.* 31 (2012) 3169–3182.
- [67] T.A. Schaedler, J.D. Thornton, I. Kruse, M. Schwarzlander, A.J. Meyer, H.W. van Veen, J. Balk, A conserved mitochondrial ATP-binding cassette transporter exports glutathione polysulfide for cytosolic metal cofactor assembly, *J. Biol. Chem.* 289 (2014) 23264–23274.
- [68] P. Gonzalez-Cabo, A. Bolinches-Amoros, J. Cabello, S. Ros, S. Moreno, H. A. Baylis, F. Palau, R.P. Vazquez-Manrique, Disruption of the ATP-binding cassette B7 (ABTM-1/ABCB7) induces oxidative stress and premature cell death in *Caenorhabditis elegans*, *J. Biol. Chem.* 286 (2011) 21304–21314.
- [69] A.P. Landry, Z. Cheng, H. Ding, Reduction of mitochondrial protein mitoNEET [2Fe–2S] clusters by human glutathione reductase, *Free Radic. Biol. Med.* 81 (2015) 119–127.
- [70] M. Lazarou, D.P. Narendra, S.M. Jin, E. Tekle, S. Banerjee, R.J. Youle, PINK1 drives Parkin self-association and HECT-like E3 activity upstream of mitochondrial binding, *J. Cell Biol.* 200 (2013) 163–172.
- [71] J. Sulston, H. J. Methods, in: *The Nematode Caenorhabditis elegans*, Cold Spring Harbour, New York, Cold Spring Harbour Laboratory Press, Cold Spring Harbour, 1988.
- [72] A. Morales-Martinez, A. Dobrzynska, P. Askjaer, Inner nuclear membrane protein LEM-2 is required for correct nuclear separation and morphology in *C. elegans*, *J. Cell Sci.* 128 (2015) 1090–1096.
- [73] C.C. Mello, J.M. Kramer, D. Stinchcomb, V. Ambros, Efficient gene transfer in *C. elegans*: extrachromosomal maintenance and integration of transforming sequences, *EMBO J.* 10 (1991) 3959–3970.
- [74] T. Miyabayashi, M.T. Palfreyman, A.E. Sluder, F. Slack, P. Sengupta, Expression and function of members of a divergent nuclear receptor family in *Caenorhabditis elegans*, *Dev. Biol.* 215 (1999) 314–331.
- [75] S. Muller, R.D. Walter, A.H. Fairlamb, Differential susceptibility of filarial and human erythrocyte glutathione reductase to inhibition by the trivalent organic arsenical melarsen oxide, *Mol. Biochem. Parasitol.* 71 (1995) 211–219.
- [76] C. Nieto, J. Almendinger, S. Gysi, E. Gomez-Orte, A. Kaech, M.O. Hengartner, R. Schnabel, S. Moreno, J. Cabello, ccz-1 mediates the digestion of apoptotic corpses in *C. elegans*, *J. Cell Sci.* 123 (2010) 2001–2007.
- [77] P.L. Larsen, P.S. Albert, D.L. Riddle, Genes that regulate both development and longevity in *Caenorhabditis elegans*, *Genetics* 139 (1995) 1567–1583.
- [78] H. Inoue, N. Hisamoto, J.H. An, R.P. Oliveira, E. Nishida, T.K. Blackwell, K. Matsumoto, The *C. elegans* p38 MAPK pathway regulates nuclear localization of the transcription factor SKN-1 in oxidative stress response, *Genes Dev.* 19 (2005) 2278–2283.
- [79] T. Etheridge, M. Rahman, C.J. Gaffney, D. Shaw, F. Shephard, J. Magudia, D. E. Solomon, T. Milne, J. Blawdziewicz, D. Constantin-Teodosiu, P.L. Greenhaff, S.A. Vanapalli, N.J. Szewczyk, The integrin-adhesome is required to maintain muscle structure, mitochondrial ATP production, and movement forces in *Caenorhabditis elegans*, *FASEB J.* 29 (2015) 1235–1246.
- [80] R.L. Krauth-Siegel, R. Blatterspiel, M. Saleh, E. Schiltz, R.H. Schirmer, R. Untucht-Grau, Glutathione reductase from human erythrocytes. The sequences of the NADPH domain and of the interface domain, *Eur. J. Biochem.* 121 (1982) 259–267.
- [81] S. Urig, J. Lieske, K. Fritz-Wolf, A. Irmeler, K. Becker, Truncated mutants of human thioredoxin reductase 1 do not exhibit glutathione reductase activity, *FEBS Lett.* 580 (2006) 3595–3600.